

Electronic Supplementary Information

Tailored Homo- and Hetero- Lanthanide Porphyrin Dimers: a Synthetic Strategy for Integrating Multiple Spintronic Functionalities into a Single Molecule

Jennifer J. Le Roy,[‡]^a Jonathan Cremers,[‡]^b Isabel A. Thomlinson,^b Michael Slota,^a William K. Myers,^c Peter H. Horton,^d Simon J. Coles,^d Harry L. Anderson^b and Lapo Bogani^a

^aDepartment of Materials, University of Oxford, Parks Rd, Oxford, OX1 3PH, UK.

^bDepartment of Chemistry, University of Oxford, Chemistry Research Laboratory, Mansfield Road, Oxford, OX1 3TA, UK.

^cCentre for Advanced ESR, Department of Chemistry, University of Oxford, Inorganic Chemistry Laboratory, South Parks Road, Oxford, OX1 3QR, UK.

^dNational Crystallography Service, School of Chemistry, University of Southampton, Southampton, SO17 1BJ, UK.

Synthetic Details	S2
X-ray Crystallography	S23
SQUID Magnetometry	S28
Electron Paramagnetic Resonance	S30
References	S34

1 Synthetic Details

1.1 General Experimental

Dry toluene and THF were obtained by passing the solvents through columns of alumina, under nitrogen. Diisopropylamine (*i*-Pr₂NH) was distilled from CaH₂ and kept over activated molecular sieves (3 Å, 8–12 mesh). Unless specified otherwise, all other solvents were used as commercially supplied. Flash chromatography was carried out on silica gel 60 under positive pressure. Analytical thin-layer chromatography was carried out on aluminum-backed silica gel 60 F254 plates. Visualization was achieved using UV light when necessary.

All UV-vis-NIR spectra were recorded in solution using a Perkin-Lambda 20 spectrometer (1 cm path length quartz cell).

Unless stated otherwise, ¹H/¹³C NMR spectra were recorded at 298 K using a Bruker AV400 (400/100 MHz) instrument. ¹H, and ¹³C NMR spectra are reported in ppm; coupling constants are given in Hertz, to the nearest 0.1 Hz. The solvent used was CDCl₃.

MALDI-ToF spectra were measured at the EPSRC National Mass Spectrometry service (Swansea) using the Applied Biosystems Voyager DE-STR or at the University of Oxford using Waters MALDI Micro MX spectrometer utilizing dithranol as a matrix.

1.2 Synthetic Procedures

The synthesis and characterization of zinc porphyrin **P1_{Zn}** and that of the capping ligand **Na[CpCo(P(O)(OEt)₂]₃** (**NaL_{OEt}**) and its precursor **Cp₂Co₃(P(O)(OEt)₂)₆** have been reported previously.¹⁻⁶ The general reaction scheme to the heterometallated dimer **P2_{Dy-Tb}** is shown in Figure S1.

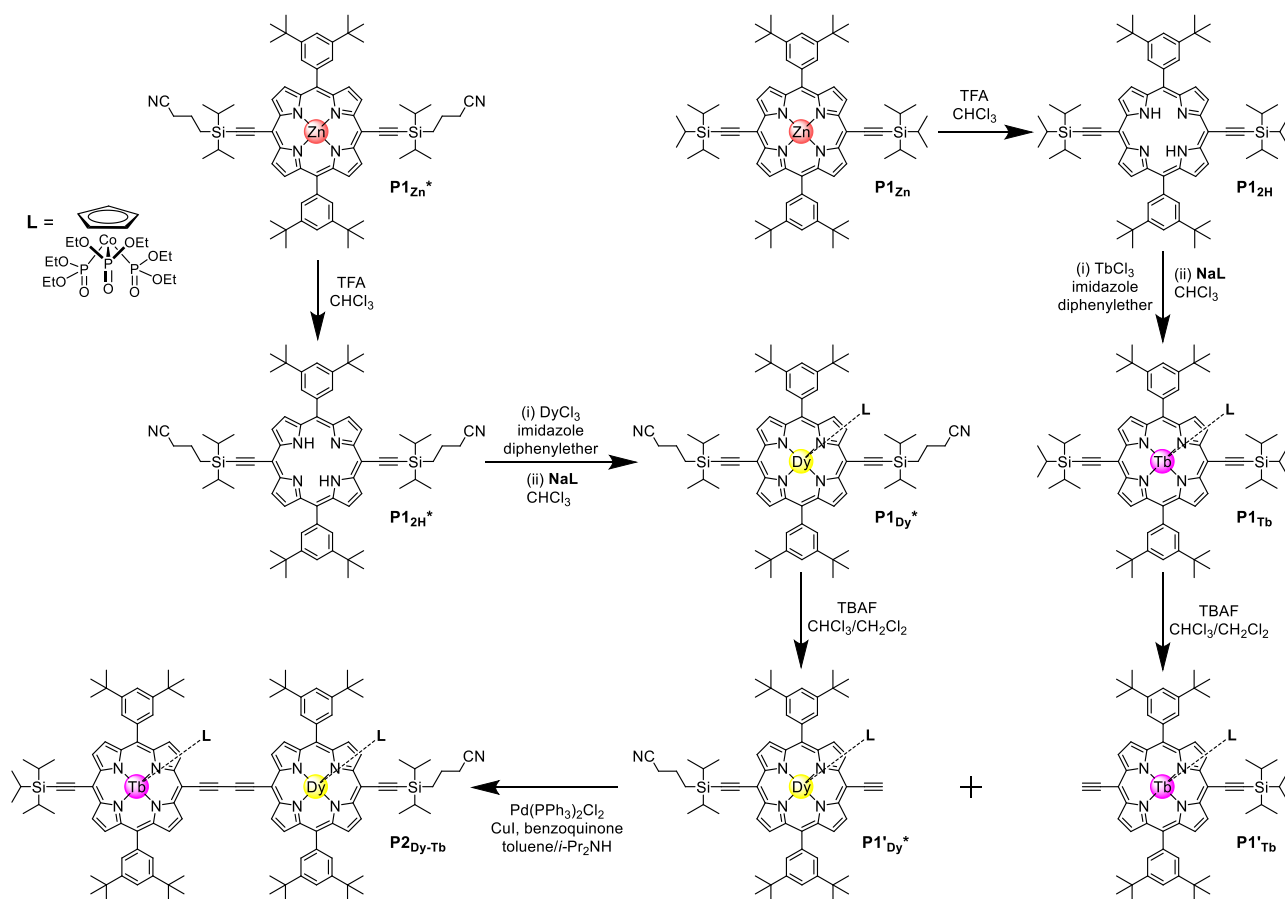
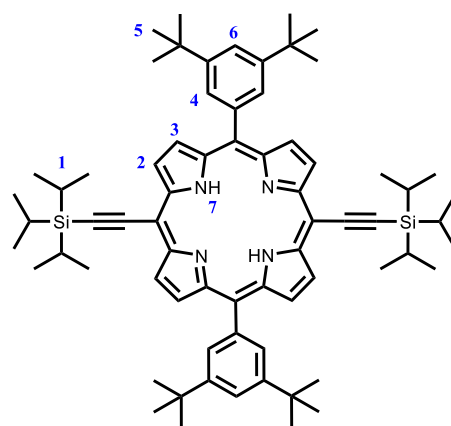


Figure S1: The general reaction scheme to **P2_{Dy-Tb}**.

P1_{2H}

P1_{Zn} (2.12 g, 1.77 mmol) was dissolved in CHCl₃ (350 mL). Trifluoroacetic acid (7.0 mL) was mixed with CHCl₃ (63 mL) to give a 10% solution. The TFA solution was added dropwise to the porphyrin solution and the reaction mixture was stirred at room temperature for 15 minutes. After the completion of the reaction, the mixture was passed immediately through a short plug of silica gel (1% pyridine in CHCl₃) and the solvents were removed. Recrystallization by layer addition (CH₂Cl₂/methanol) gave the product as a dark blue-green solid (1.76 g, 96%).



Crystals of **P1_{2H}** suitable for X-ray diffraction were obtained by layer addition of methanol to a solution of the porphyrin in DCM.

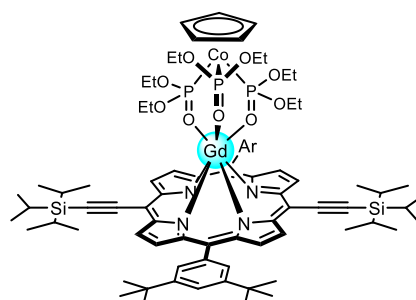
¹H NMR (400 MHz, CDCl₃, 298 K): δ_H (ppm) 9.65 (4H, d, *J* = 4.7 Hz, H₂), 8.87 (4H, d, *J* = 4.7 Hz, H₃), 8.02 (4H, d, *J* = 1.8 Hz, H₄), 7.81 (2H, t, *J* = 1.8 Hz, H₆), 1.55 (42H, s, H₅), 1.39-1.42 (36H, m, H₁), -2.10 (2H, s, H₇).

MALDI-TOF: *m/z* = 1049 (C₇₀H₉₄N₄Si₂, M⁺ requires 1047).

λ_{max} (CHCl₃) / nm log(ϵ): 439 (5.65), 448 (5.41), 584 (4.14), 622 (4.41), 637 (4.60).

P1_{Gd}

In a dry Schlenk flask, free-base porphyrin (**P1_{2H}**) (50 mg, 47.7 μmol), anhydrous GdCl₃ (126 mg, 0.47 mmol), diphenyl ether (1.0 g) and imidazole (1.0 g) were heated to 220 °C for 3 h. The mixture was allowed to cool to room temperature after which CHCl₃ (25 mL) was added and the mixture was washed with water to remove the imidazole. The CHCl₃ layer was dried over magnesium sulfate and the solvent was removed. The diphenyl ether was then removed by vacuum distillation utilizing a Hickmann apparatus. The residue was dissolved in CHCl₃ (5 mL), NaOEt (26.8 mg, 47.7 μmol) was added and the mixture was stirred at room temperature for 30 min. The reaction mixture was passed through a short plug of silica gel (CHCl₃). Recrystallization by layer addition (CH₂Cl₂/methanol) gave the product as a dark blue-green solid (51.7 mg, 62%).



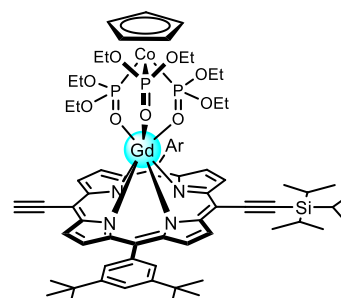
Crystals of **P1_{Gy}** suitable for X-ray diffraction were obtained by layer addition of methanol to a solution of the porphyrin in chlorobenzene.

MALDI-TOF: *m/z* = 1739 (C₈₇H₁₂₇CoGdN₄O₉P₃Si₂, M⁺ requires 1738).

λ_{max} (CHCl₃) / nm log(ϵ): 443 (5.67), 453 (5.45), 588 (4.17), 624 (4.29), 639 (4.77).

P1'_{Gd}

P1_{Gd} (108 mg, 0.22 mmol) was dissolved in CHCl₃ (2 mL) and CH₂Cl₂ (8 mL). Tetra-*n*-butylammonium fluoride (1.0 mL, 1.0 M solution in THF, 1.0 mmol) was added to the stirred solution in small portions. The progress of the reaction was monitored by TLC (petrol ether:ethyl acetate:pyridine = 10:1:1) until an optimal mixture was reached (90



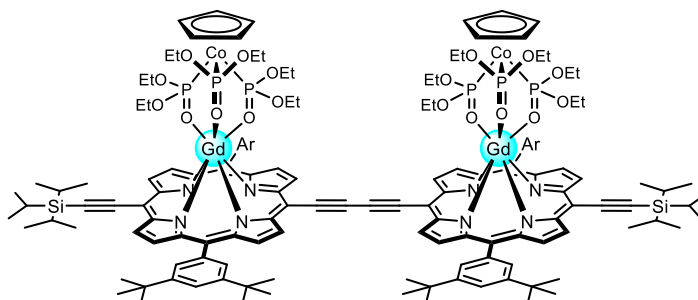
min). The mixture was passed through a short plug of silica gel (CHCl₃). The reaction mixture was purified by silica gel chromatography (petrol ether:CHCl₃ = 1:1 → 0:1). Recrystallization by layer addition (CH₂Cl₂/methanol) gave the product as a dark blue-green solid (18.4 mg, 19%).

MALDI-TOF: $m/z = 1582$ (C₇₈H₁₀₇CoGdN₄O₉P₃Si, M⁺ requires 1582).

λ_{max} (CHCl₃) / nm log(ϵ): 442 (5.70), 453 (5.47), 587 (4.19), 624 (4.31), 640 (4.78).

P2_{Gd2}

P1'_{Gd} (24.4 mg, 15.4 μ mol) was dissolved in toluene (1 mL). A catalyst solution was prepared by dissolving Pd(PPh₃)₂Cl₂ (1.1 mg, 1.5 μ mol), CuI (2.9 mg, 15.4 μ mol) and 1,4-benzoquinone (2.2 mg, 20.5 μ mol) in toluene (0.86 mL) and *i*-



Pr₂NH (0.14 mL). The catalyst solution was added to the reaction mixture. The reaction mixture was stirred at room temperature for 30 min and passed through a short silica gel column (CHCl₃). The reaction mixture was purified by silica gel chromatography (petrol ether:CHCl₃ = 1:1 → 0:1). Recrystallization by layer addition (CH₂Cl₂/methanol) gave the product as a dark blue-green solid (17.4 mg, 71%).

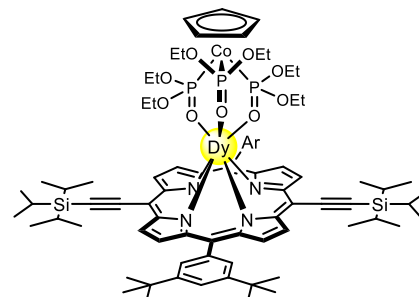
Crystals of **P2**_{Gd2} suitable for X-ray diffraction were obtained by dissolving the dimer in a one-to-one mixture of DCM and ethanol. Slow evaporation of the DCM allowed the dimer to slowly crystallize over time.

MALDI-TOF: $m/z = 3162$ (C₁₅₆H₂₁₂Co₂Gd₂N₈O₁₈P₆Si₂, M⁺ requires 3161).

λ_{max} (CHCl₃) / nm log(ϵ): 435 (5.28), 460 (5.55), 496 (5.34), 586 (4.35), 667 (4.88), 733 (5.10).

P1_{Dy}

In a dry Schlenk flask, free-base porphyrin (**P1**_{2H}) (200 mg, 0.19 mmol), anhydrous DyCl₃ (513 mg, 1.91 mmol), diphenyl ether (4.0 g) and imidazole (4.0 g) were heated to 220 °C for 3 h. The mixture was allowed to cool to room temperature after which CHCl₃ (50 mL) was added and the mixture was washed with water to remove the imidazole. The CHCl₃ layer was dried over magnesium sulfate and the solvent was removed. The diphenyl ether was then removed by



vacuum distillation utilizing a Hickmann apparatus. The residue was dissolved in CHCl_3 (20 mL), NaLOEt (104 mg, 0.19 mmol) was added and the mixture was stirred at room temperature for 30 min. The reaction mixture was passed through a short plug of silica gel (CHCl_3). Recrystallization by layer addition (CH_2Cl_2 /methanol) gave the product as a dark blue-green solid (235 mg, 71%).

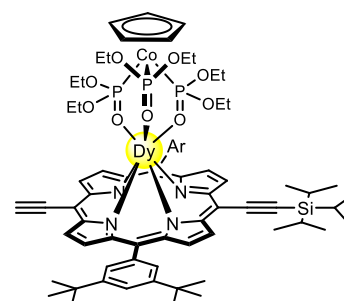
Crystals of P1_{Dy} suitable for X-ray diffraction were obtained by layer addition of methanol to a solution of the porphyrin in chlorobenzene.

MALDI-TOF: $m/z = 1744$ ($\text{C}_{87}\text{H}_{127}\text{CoN}_4\text{O}_9\text{P}_3\text{Si}_2\text{Dy}$, M^+ requires 1744).

λ_{max} (CHCl_3) / nm $\log(\epsilon)$: 443 (5.68), 453 (5.47), 587 (4.20), 624 (4.33), 637 (4.78).

$\text{P1}'_{\text{Dy}}$

P1_{Dy} (230 mg, 0.13 mmol) was dissolved in CHCl_3 (2 mL) and CH_2Cl_2 (10 mL). Tetra-*n*-butylammonium fluoride (1.0 mL, 1.0 M solution in THF, 1.0 mmol) was added to the stirred solution in small portions. The progress of the reaction was monitored by TLC (petrol ether:ethyl acetate:pyridine = 10:1:1) until an optimal mixture was reached (60 min). The mixture was passed through a short plug of silica gel (CHCl_3). The reaction mixture was purified by silica gel chromatography (petrol ether: CHCl_3 = 1:1 \rightarrow 0:1). Recrystallization by layer addition (CH_2Cl_2 /methanol) gave the product as a dark blue-green solid (52.7 mg, 25%).

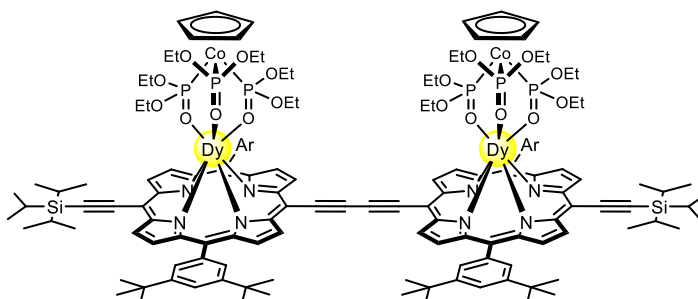


MALDI-TOF: $m/z = 1588$ ($\text{C}_{78}\text{H}_{107}\text{CoDyN}_4\text{O}_9\text{P}_3\text{Si}$, M^+ requires 1588).

λ_{max} (CHCl_3) / nm $\log(\epsilon)$: 441 (5.54), 450 (5.42), 583 (4.16), 632 (4.59).

$\text{P2}_{\text{Dy}2}$

$\text{P1}'_{\text{Dy}}$ (52.7 mg, 33.3 μmol) was dissolved in toluene (2 mL). A catalyst solution was prepared by dissolving $\text{Pd}(\text{PPh}_3)_2\text{Cl}_2$ (2.3 mg, 3.3 μmol), CuI (6.3 mg, 33.3 μmol) and 1,4-benzoquinone (4.8 mg, 44.3 μmol) in toluene (2.1 mL) and *i*- Pr_2NH (0.35 mL). The catalyst solution was added to the reaction mixture. The reaction mixture was stirred at room temperature for 1 h and passed through a short silica gel column (CHCl_3). The reaction mixture was purified by silica gel chromatography (petrol ether: CHCl_3 = 1:1 \rightarrow 0:1).



Recrystallization by layer addition (CH₂Cl₂/methanol) gave the product as a dark blue-green solid (25.1 mg, 48%).

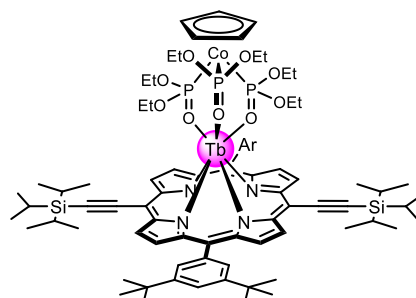
Crystals of **P2_{Dy2}** suitable for X-ray diffraction were obtained by dissolving the dimer in a one-to-one mixture of DCM and ethanol. Slow evaporation of the DCM allowed the dimer to slowly crystallize over time.

MALDI-TOF: $m/z = 3172$ (C₁₅₆H₂₁₂Co₂Dy₂N₈O₁₈P₆Si₂, M⁺ requires 3172).

λ_{max} (CHCl₃) / nm log(ϵ): 435 (5.27), 460 (5.55), 496 (5.30), 584 (4.32), 666 (4.87), 731 (5.07).

P1_{Tb}

In a dry Schlenk flask, free-base porphyrin (**P1_{2H}**) (200 mg, 0.19 mmol), TbCl₃·6H₂O (710 mg, 1.91 mmol), diphenyl ether (4.0 g) and imidazole (4.0 g) were heated to 190 °C for 2 h. The mixture was allowed to cool to room temperature after which CHCl₃ (50 mL) was added and the mixture was washed with water to remove the imidazole. The CHCl₃ layer was dried over sodium sulfate and the solvent was removed. The diphenyl ether was then removed by vacuum distillation utilizing a Hickmann apparatus. The residue was dissolved in CHCl₃ (5 mL), Na₁OEt (109 mg, 0.19 mmol) was added and the mixture was stirred at room temperature for 17 h. The reaction mixture was concentrated and purified by silica gel column chromatography (petroleum ether : ethyl acetate : pyridine = 20 : 1 : 1). Recrystallization by layer addition (CH₂Cl₂/methanol) gave the product as a dark blue-green solid (203 mg, 61%).



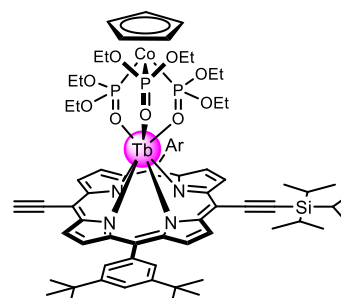
Crystals of **P1_{Tb}** suitable for X-ray diffraction were obtained by layer addition of methanol to a solution of the porphyrin in chlorobenzene.

MALDI-TOF: $m/z = 1740$ (C₈₇H₁₂₇CoN₄O₉P₃Si₂Tb, M⁺ requires 1740).

λ_{max} (CHCl₃) / nm log(ϵ): 440 (5.71), 579 (4.24), 626 (4.36).

P1'_{Tb}

P1_{Tb} (143 mg, 82 μ mol) was dissolved in CHCl₃ (1 mL) and CH₂Cl₂ (5 mL). Tetra-*n*-butylammonium fluoride (0.12 mL, 1.0 M solution in THF, 0.12 mmol) was added to the stirred solution in small portions. The progress of the reaction was monitored by TLC (petrol ether:ethyl acetate:pyridine = 10:1:1) until an optimal mixture was reached (80



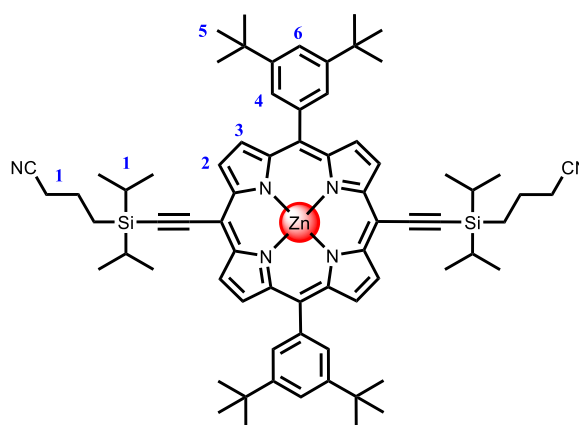
min). The mixture was passed through a short plug of silica gel (CHCl₃). The reaction mixture was purified by silica gel chromatography (petrol ether:ethyl acetate:pyridine = 20:1:1 → 10:1:1). Recrystallization by layer addition (CH₂Cl₂/methanol) gave the product as a dark blue-green solid (65.1 mg, 50%).

MALDI-TOF: $m/z = 1584$ (C₇₈H₁₀₇CoN₄O₉P₃SiTb, M⁺ requires 1583).

λ_{max} (CHCl₃) / nm log(ϵ): 442 (5.76), 580 (4.27), 628 (4.41).

P1_{Zn}*

tris-(Dibenzylideneacetone)-di-palladium(0) (50.4 mg, 55 mmol), copper(I) iodide (21.0 mg, 0.11 mmol), triphenylphosphine (28.9 mg, 0.11 mmol) and dibromoporphyrin (500 mg, 0.55 mmol) were placed in a dried two-neck roundbottom flask under argon. Toluene (35 mL), *i*-Pr₂NH (19 mL) and pyridine (1 mL) were added and the reaction mixture was deoxygenated.



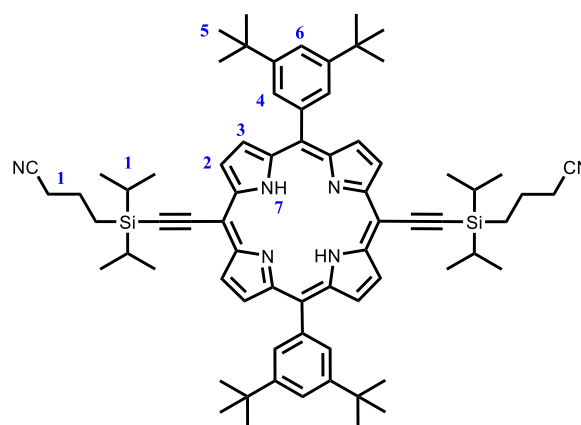
Cyanopropyldiisopropylsilyl acetylene (343 mg, 1.65 mmol) was added by syringe. The reaction mixture was stirred at 50 °C for 2 h, and monitored by TLC. The solvents were removed and the residue was passed through a short silica gel plug using CH₃Cl containing 1% pyridine. The reaction mixture was purified by silica gel chromatography (petrol ether:ethyl acetate:pyridine = 10:1:1). Recrystallization by layer addition (CH₂Cl₂/methanol) gave the product as a dark blue-green solid (201 mg, 31%).

Crystals of P1_{Zn}* suitable for X-ray diffraction were obtained by layer addition of methanol to a solution of the porphyrin in DCM.

¹H NMR (400 MHz, CDCl₃, 298 K): δ_H (ppm) 9.64 (4H, d, $J = 4.6$ Hz, H2), 8.92 (4H, d, $J = 4.6$ Hz, H3), 7.99 (4H, d, $J = 1.8$ Hz, H4), 7.80 (2H, t, $J = 1.8$ Hz, H6), 1.55 (36H, s, H5), 2.57-0.92 (40H, m, H1).

MALDI-TOF: $m/z = 1161$ (C₇₂H₉₀N₆Si₂Zn, M⁺ requires 1161).

λ_{max} (CHCl₃) / nm log(ϵ): 439 (5.65), 448 (5.41), 584 (4.14), 622 (4.41), 637 (4.60).



P1_{2H}*

P1_{2n}* (201 mg, 0.172 mmol) was dissolved in CHCl₃ (33 mL). Trifluoroacetic acid (0.68 mL) was mixed with CHCl₃ (6 mL) to give a 10% solution. The TFA solution was added dropwise to the porphyrin solution and the reaction mixture was stirred at room temperature for 15 minutes. The reaction mixture was passed through a short plug of silica gel (CHCl₃). Recrystallization by layer addition (CH₂Cl₂/methanol) gave the product as a dark blue-green solid (147 mg, 78%).

Crystals of **P1_{2H}** suitable for X-ray diffraction were obtained by layer addition of methanol to a solution of the porphyrin in DCM.

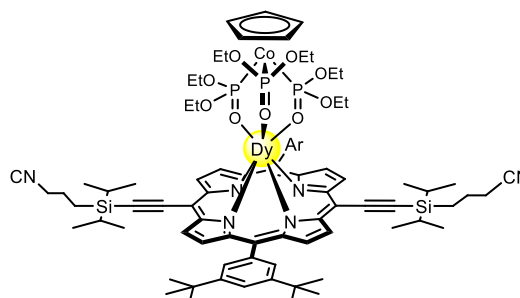
¹H NMR (400 MHz, CDCl₃, 298 K): δ_H (ppm) 9.61 (4H, d, *J* = 4.7 Hz, H2), 8.89 (4H, d, *J* = 4.7 Hz, H3), 8.02 (4H, d, *J* = 1.8 Hz, H4), 7.82 (2H, t, *J* = 1.8 Hz, H6), 1.55 (42H, s, H5), 2.62-0.76 (40H, m, H1), -2.12 (2H, s, H7).

λ_{max} (CHCl₃) / nm log(ε): 434 (5.65), 441 (5.55), 510 (3.88), 544 (4.18), 585 (4.78), 622 (3.90), 680 (4.43).

MALDI-TOF: *m/z* = 1097 (C₇₂H₉₂N₆Si₂, M⁺ requires 1098).

P1_{Dy}*

In a dry Schlenk flask, free-base porphyrin (**P1_{2H}***) (100 mg, 0.09 mmol), anhydrous DyCl₃ (343 mg, 0.91 mmol), diphenyl ether (2.0 g) and imidazole (2.0 g) were heated to 210 °C for 3 h. The mixture was allowed to cool to room temperature after which CHCl₃ (100 mL)



was added and the mixture was washed with water to remove the imidazole. The CHCl₃ layer was dried over sodium sulfate and the solvent was removed. The diphenyl ether was then removed by vacuum distillation utilizing a Hickmann apparatus. The residue was dissolved in CHCl₃ (2.5 mL), **NaLOEt** (51 mg, 0.09 mmol) was added and the mixture was stirred at room temperature for 16 h. The reaction mixture was passed through a short plug of silica gel (CHCl₃). Recrystallization by layer addition (CH₂Cl₂/methanol) gave the product as a dark blue-green solid (21.4 mg, 13%).

Crystals of **P1_{Dy}*** suitable for X-ray diffraction were obtained by layer addition of methanol to a solution of the porphyrin in chlorobenzene.

MALDI-TOF: *m/z* = 1794 (C₈₉H₁₂₅CoDyN₆O₉P₃Si₂, M⁺ requires 1794).

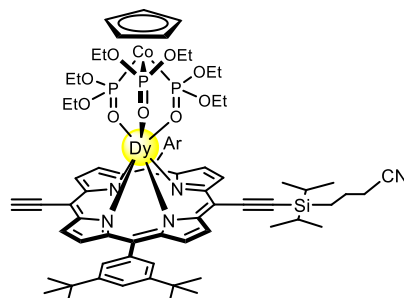
λ_{max} (CHCl₃) / nm log(ϵ): 442 (5.67), 452 (5.43), 587 (4.15), 624 (4.33), 638 (4.72).

P1'_{Dy}*

P1_{Dy}* (21.4 mg, 13 μ mol) was dissolved in CH₂Cl₂ (1 mL) and CHCl₃ (1 mL). Tetra-*n*-butylammonium fluoride (18 μ L, 1.0 M solution in THF, 18 μ mol) was added to the stirred solution in small portions.

The progress of the reaction was monitored by TLC (petrol ether:ethyl acetate:pyridine = 10:1:1) until an optimal mixture was reached (60 min). The mixture was passed through a short plug of silica gel (CHCl₃).

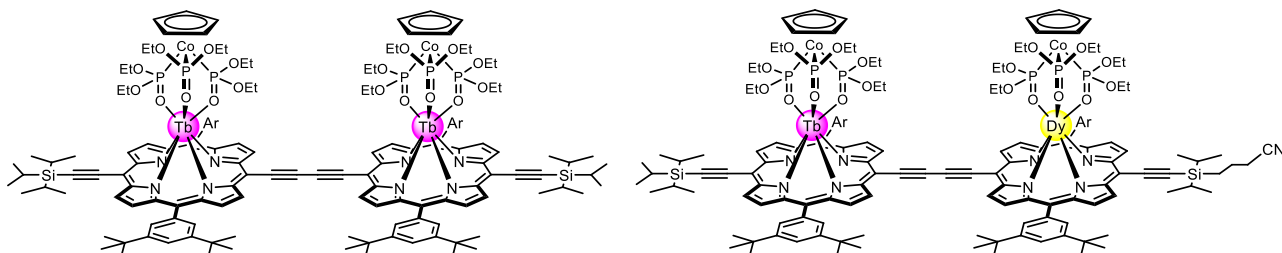
The reaction mixture was purified by silica gel chromatography (petrol ether:ethyl acetate:pyridine = 20:1:1 \rightarrow 10:1:1). Recrystallization by layer addition (CH₂Cl₂/methanol) gave the product as a dark blue-green solid (8.4 mg, 44%).



MALDI-TOF: m/z = 1613 (C₇₉H₁₀₆CoDyN₅O₉P₃Si, M⁺ requires 1613).

λ_{max} (CHCl₃) / nm log(ϵ): 444 (5.68), 453 (5.41), 588 (4.18), 626 (4.35), 639 (4.73).

P2_{Tb2} and P2_{Dy-Tb}



P1'_{Dy}* (8.4 mg, 5.2 μ mol) and **P1'_{Tb}** (65.1 mg, 41.9 μ mol) was dissolved in toluene (2.5 mL). A catalyst solution was prepared by dissolving Pd(PPh₃)₂Cl₂ (3.3 mg, 4.7 μ mol), CuI (9.0 mg, 47.1 μ mol) and 1,4-benzoquinone (6.8 mg, 62.8 μ mol) in toluene (3 mL) and *i*-Pr₂NH (0.5 mL). The catalyst solution was added to the reaction mixture. The reaction mixture was stirred at room temperature for 1 h and passed through a short silica gel column (CHCl₃). The two formed dimers were separated by silica gel chromatography (cyclohexane:CH₂Cl₂ = 1:1 \rightarrow 0:1). **P2_{Tb2}** was recrystallised by layer addition of methanol to a solution in CH₂Cl₂, to give the product as a dark blue-green solid (21.4 mg, 33%, yield calculated from P1'_{Tb}). **P2_{Dy-Tb}** was also recrystallised from CH₂Cl₂/methanol to give the product as a dark blue solid (4.1 mg, 25%, yield calculated from P1'_{Dy}*). The reaction also generated a small amount of **P2_{Dy2}*** but this product was not isolated.

MALDI-TOF P2_{Tb2}: m/z = 3165 (C₁₅₆H₂₁₂Co₂N₈O₁₈P₆Si₂Tb₂, M⁺ requires 3165).

MALDI-TOF P2_{Dy-Tb}: m/z = 3194 (C₁₅₇H₂₁₂Co₂DyN₉O₁₈P₆Si₂Tb, M⁺ requires 3193).

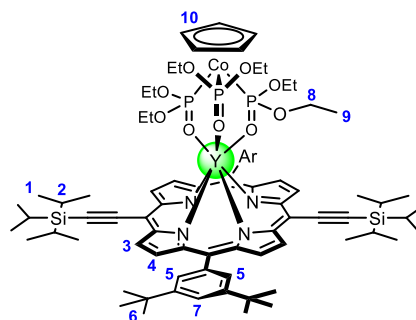
λ_{max} **P2_{Tb2}** (CHCl₃) / nm log(ϵ): 435 (5.25), 460 (5.55), 496 (5.30), 584 (4.33), 666 (4.99), 731 (5.14).

λ_{max} **P2_{Dy-Tb}** (CHCl₃) / nm log(ϵ): 435 (5.25), 460 (5.55), 496 (5.29), 584 (4.34), 666 (4.86), 731 (5.06).

P1_Y

A diamagnetic yttrium analogue was prepared to investigate the structure of a capped porphyrin by ¹H-NMR spectroscopy.

In a dry Schlenk flask, free-base porphyrin (**P1_{2H}**) (100 mg, 0.10 mmol), YCl₃·6H₂O (289 mg, 0.95 mmol), diphenyl ether (2.0 g) and imidazole (2.0 g) were heated to 220 °C for 2 h. The mixture was allowed to cool to room temperature after which



CHCl₃ (50 mL) was added and the mixture was washed with water to remove the imidazole. The CHCl₃ layer was dried over sodium sulfate and the solvent was removed. The diphenyl ether was then removed by vacuum distillation utilizing a Hickmann apparatus. The residue was dissolved in CHCl₃ (2.5 mL), NaOEt (51 mg, 0.10 mmol) was added and the mixture was stirred at room temperature for 1 h. The reaction mixture was concentrated and purified by silica gel column chromatography (petroleum ether : ethyl acetate : pyridine = 20 : 1 : 1). Recrystallization by layer addition (CH₂Cl₂/methanol) gave the product as a dark blue-green solid (111 mg, 70%).

Crystals of **P1_Y** suitable for X-ray diffraction were obtained by layer addition of methanol to a solution of the porphyrin in chlorobenzene.

¹H NMR (400 MHz, CDCl₃, 298 K): δ_H (ppm) 9.57 (4H, d, J = 4.5 Hz, H3), 8.72 (4H, d, J = 4.5 Hz, H4), 8.28 (2H, t, J = 1.6 Hz, H5), 7.75 (2H, t, J = 1.8 Hz, H7), 7.63 (2H, t, J = 1.5 Hz, H5), 4.11 (5H, s, H10), 2.64 (6H, m, H8), 2.54 (6H, m, H8), 1.63 (18H, s, H1), 1.43 (42H, s, H2 and H6), 0.77 (18H, t, J = 7.1 Hz, H9).

λ_{max} (CHCl₃) / nm log(ϵ): 443 (5.67), 453 (5.43), 588 (4.17), 624 (4.29), 639 (4.78).

1.3 Spectra Confirming Identity of New Compounds

P1_{Gd}

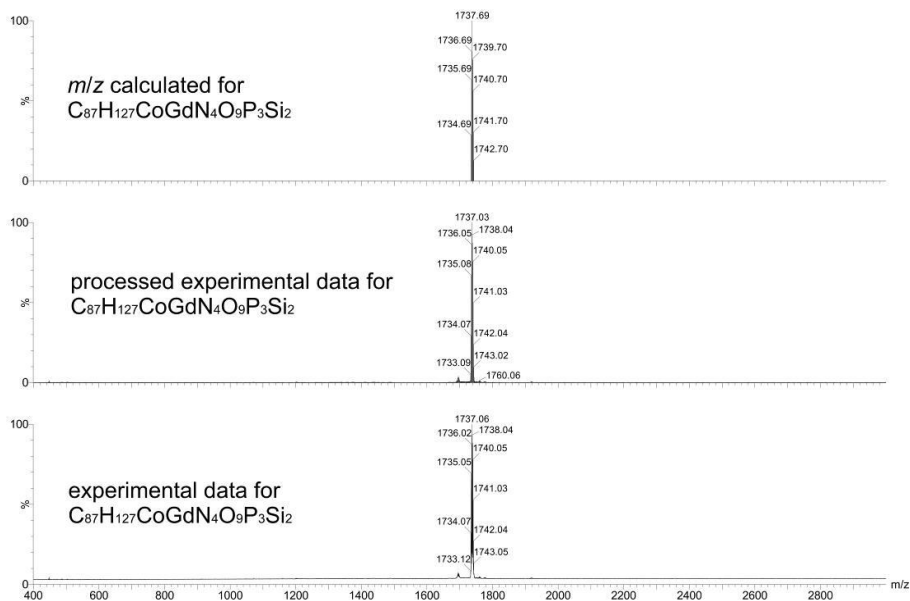


Figure S2. The full MALDI-MS spectrum of P1_{Gd} ($m/z = 1737$ (C₈₇H₁₂₇CoGdN₄O₉P₃Si₂, M⁺ requires 1738), matrix: dithranol).

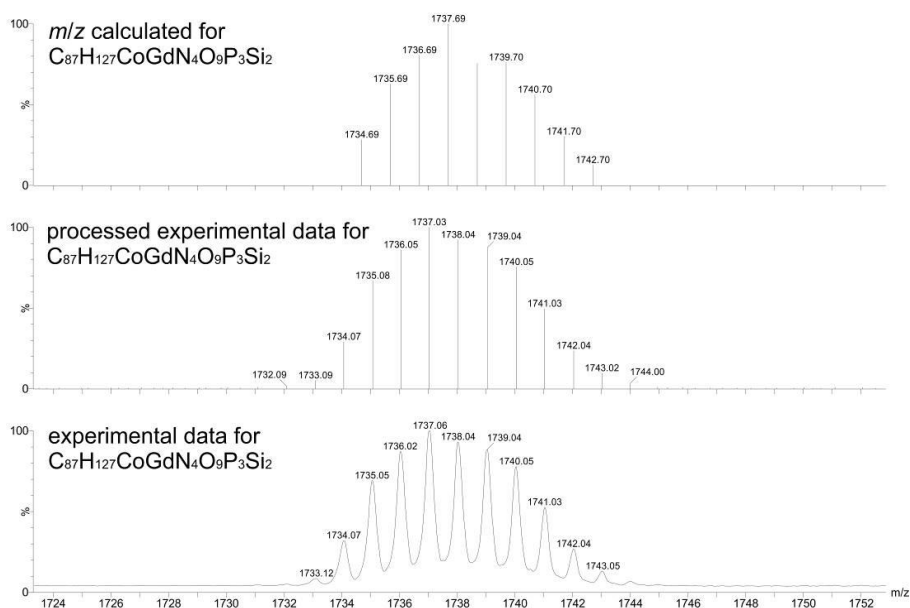


Figure S3. Zoom-in of the MALDI-MS spectrum of P1_{Gd} ($m/z = 1737$ (C₈₇H₁₂₇CoGdN₄O₉P₃Si₂, M⁺ requires 1738), matrix: dithranol).

P2_{Gd2}

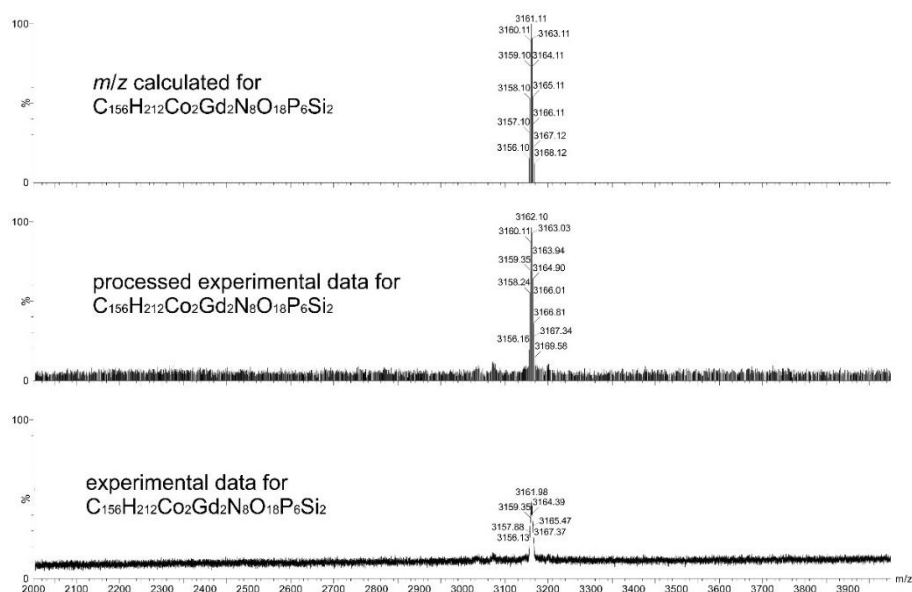


Figure S4. The full MALDI-MS spectrum of P2_{Gd2} ($m/z = 3162$ (C₁₅₆H₂₁₂Co₂Gd₂N₈O₁₈P₆Si₂, M⁺ requires 3161), matrix: dithranol).

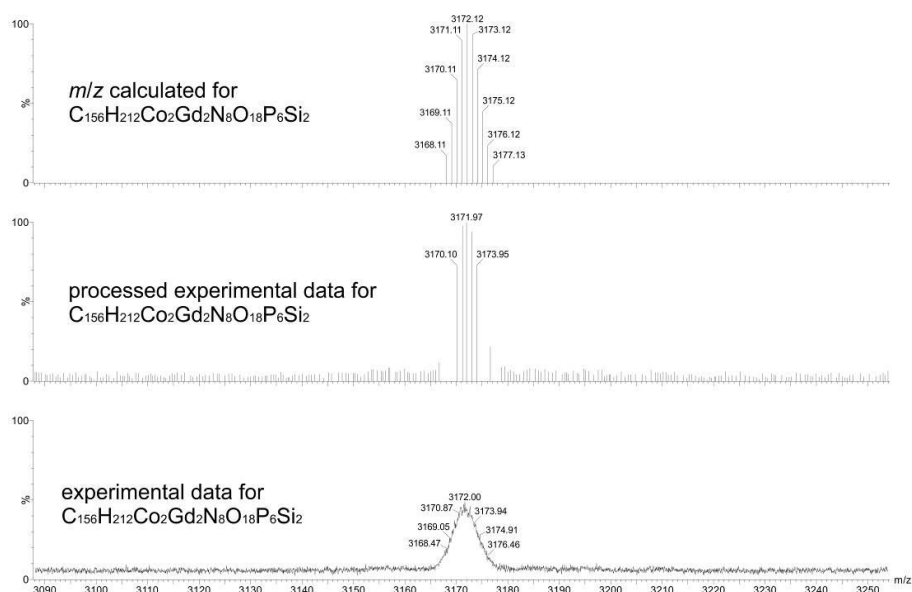


Figure S5. Zoom-in of the MALDI-MS spectrum of P2_{Gd2} ($m/z = 3162$ (C₁₅₆H₂₁₂Co₂Gd₂N₈O₁₈P₆Si₂, M⁺ requires 3161), matrix: dithranol).

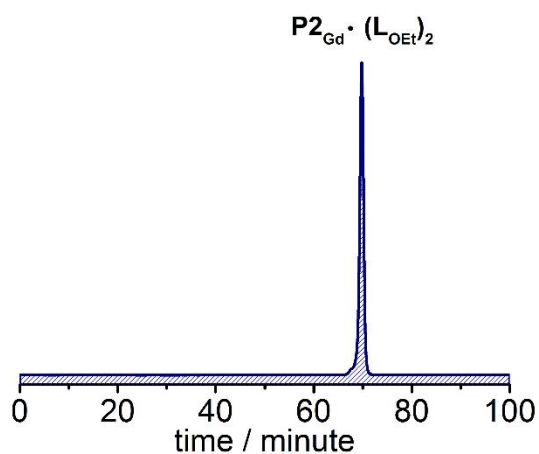


Figure S6. Analytical GPC trace (PLGel columns, toluene + 1% pyridine, detection at 731 nm) of **P2_{Gd2}**.

P1_{Dy}

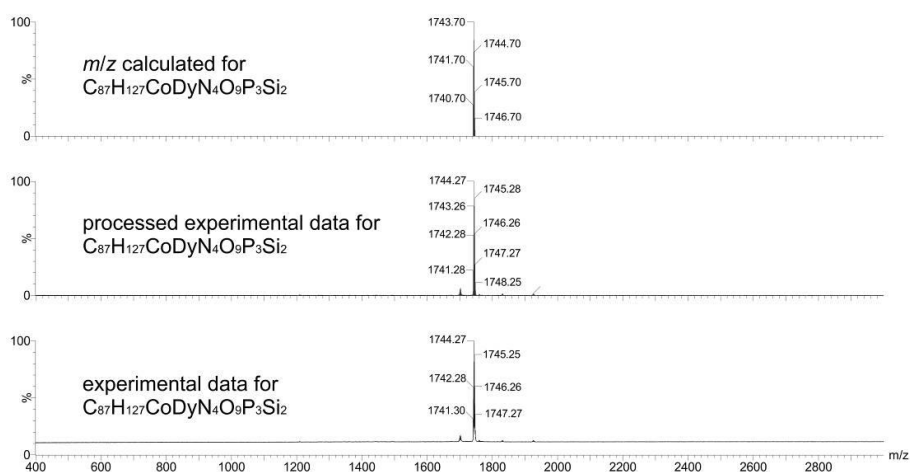


Figure S7. The full MALDI-MS spectrum of **P1_{Dy}** ($m/z = 1744$ ($C_{87}H_{127}CoDyN_4O_9P_3Si_2$, M^+ requires 1744), matrix: dithranol).

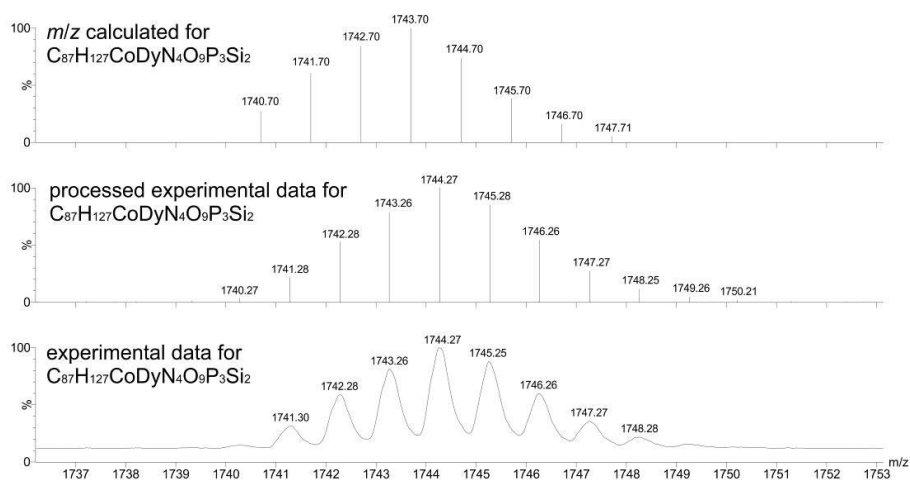


Figure S8. Zoom-in of the MALDI-MS spectrum of **P1_{Dy}** ($m/z = 1744$ ($C_{87}H_{127}CoDyN_4O_9P_3Si_2$, M^+ requires 1744), matrix: dithranol).

P2_{Dy2}

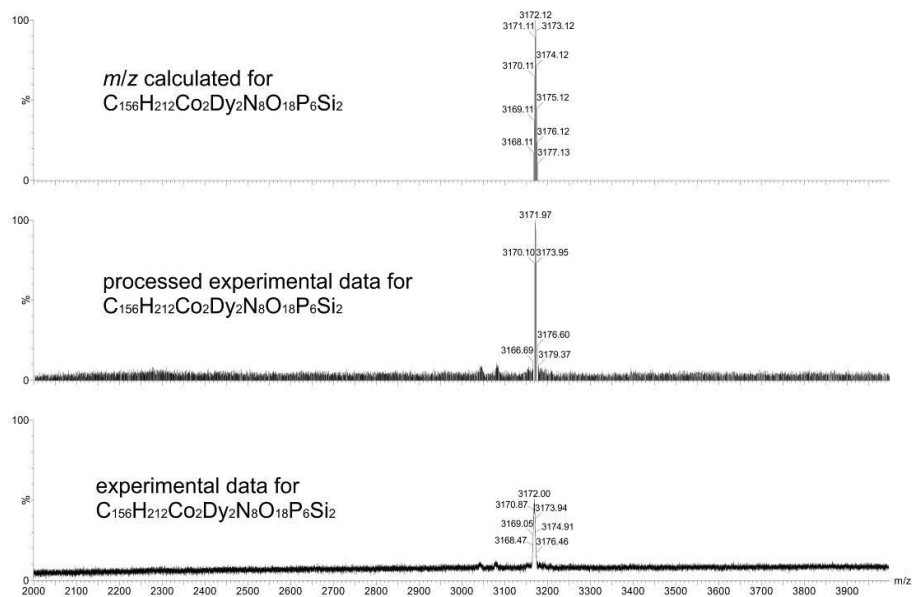


Figure S9. The full MALDI-MS spectrum of **P2_{Dy2}** ($m/z = 3172$ (C₁₅₆H₂₁₂Co₂Dy₂N₈O₁₈P₆Si₂, M⁺ requires 3172), matrix: dithranol).

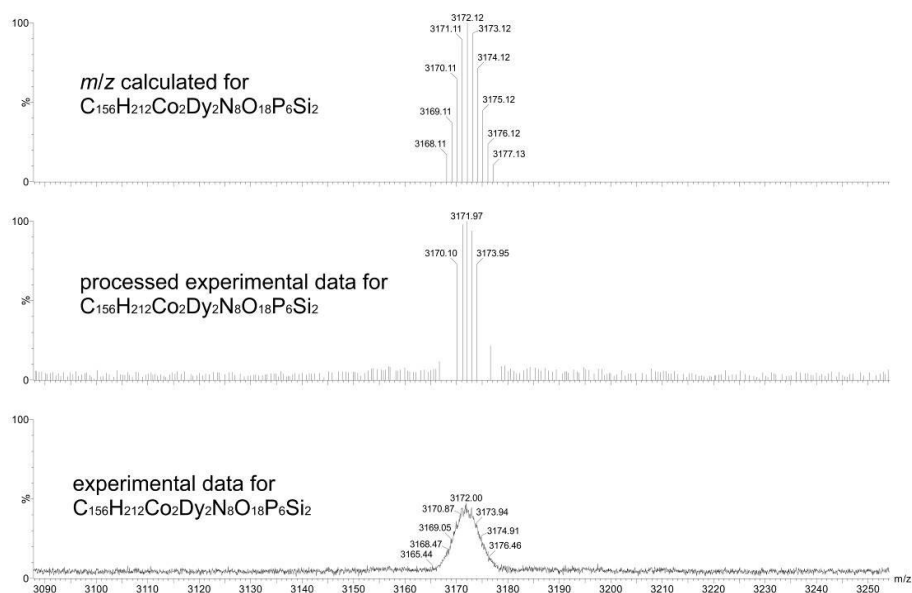


Figure S10. Zoom-in of the MALDI-MS spectrum of **P2_{Dy2}** ($m/z = 3172$ (C₁₅₆H₂₁₂Co₂Dy₂N₈O₁₈P₆Si₂, M⁺ requires 3172), matrix: dithranol).

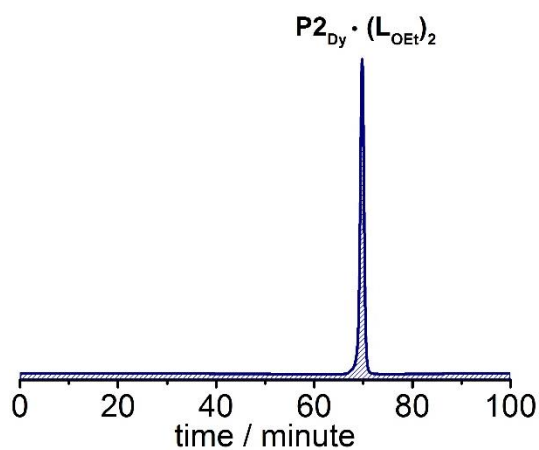


Figure S11. Analytical GPC trace (PLGel columns, toluene + 1% pyridine, detection at 731 nm) of **P2_{Dy}**.

P1_{Tb} · (LOEt)

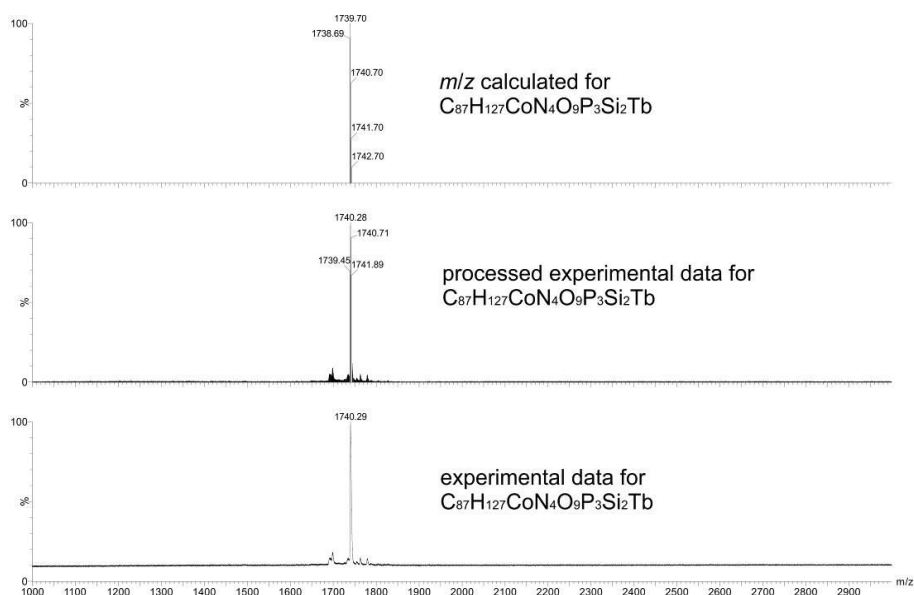


Figure 12: The full MALDI-MS spectrum of **P1_{Tb}** ($m/z = 1740$ ($C_{87}H_{127}CoN_4O_9P_3Si_2Tb$, M^+ requires 1740), matrix: dithranol).

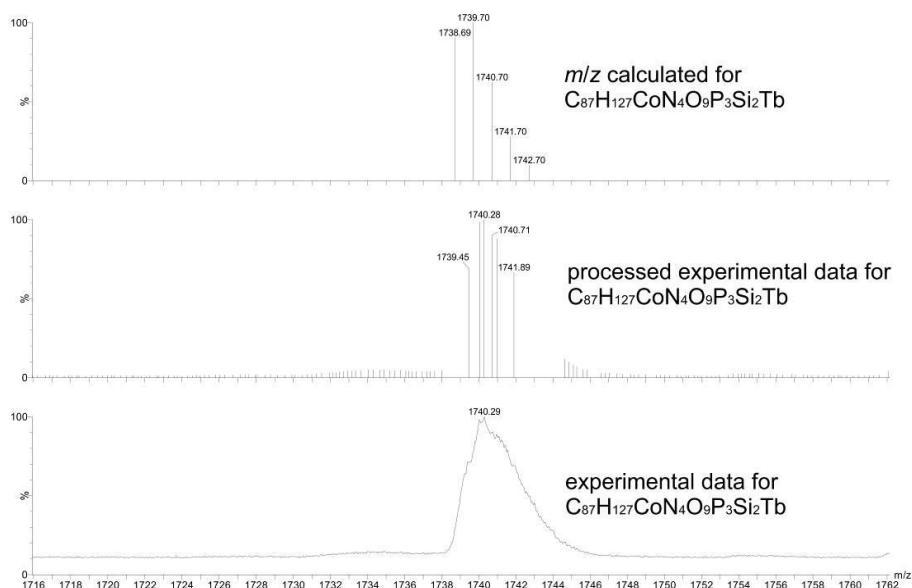


Figure S13. Zoom-in of the MALDI-MS spectrum of **P1_{Tb}** ($m/z = 1740$ ($C_{87}H_{127}CoN_4O_9P_3Si_2Tb$, M^+ requires 1740), matrix: dithranol).

P1'_{Tb}

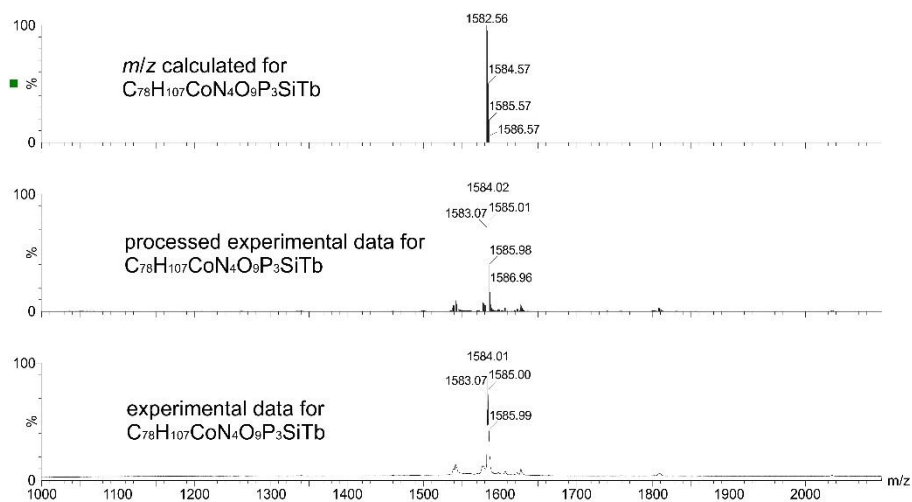


Figure S14. The full MALDI-MS spectrum of **P1'_{Tb}** ($m/z = 1584$ ($C_{78}H_{107}CoN_4O_9P_3SiTb$, M^+ requires 1583), matrix: dithranol).

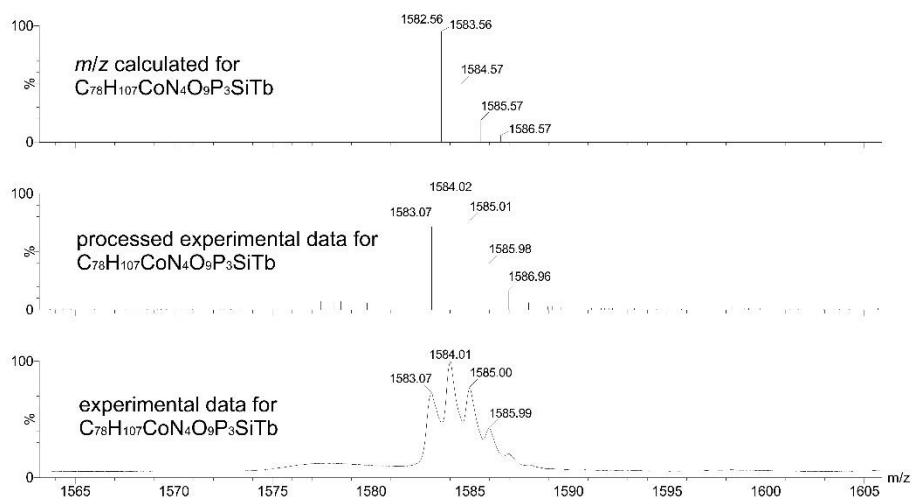


Figure S15. Zoom-in of the MALDI-MS spectrum of **P1'_{Tb}** ($m/z = 1584$ ($C_{78}H_{107}CoN_4O_9P_3SiTb$, M^+ requires 1583), matrix: dithranol).

P2_{Tb2}

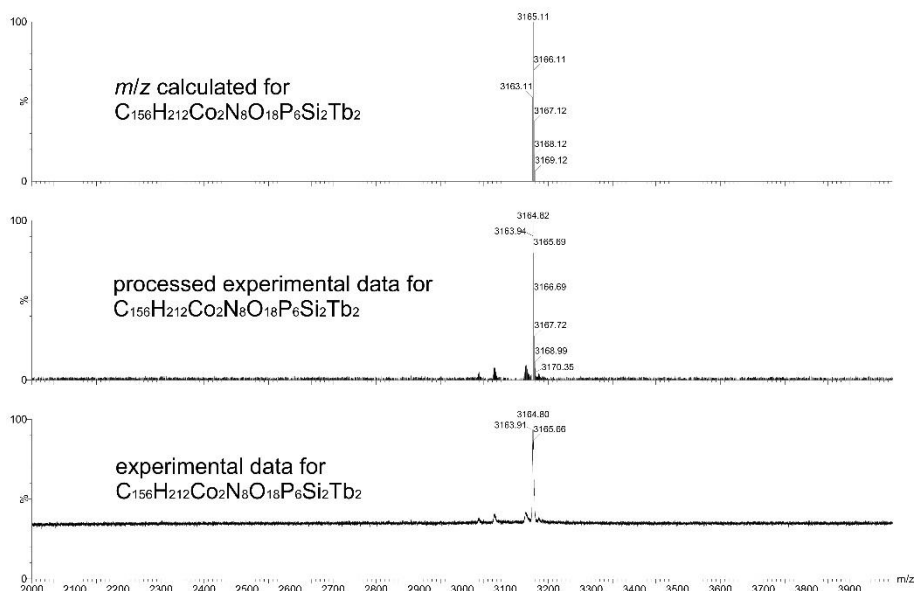


Figure S16. The full MALDI-MS spectrum of **P2_{Tb2}** ($m/z = 3165$ ($C_{156}H_{212}Co_2N_8O_{18}P_6Si_2Tb_2$, M^+ requires 3165), matrix: dithranol).

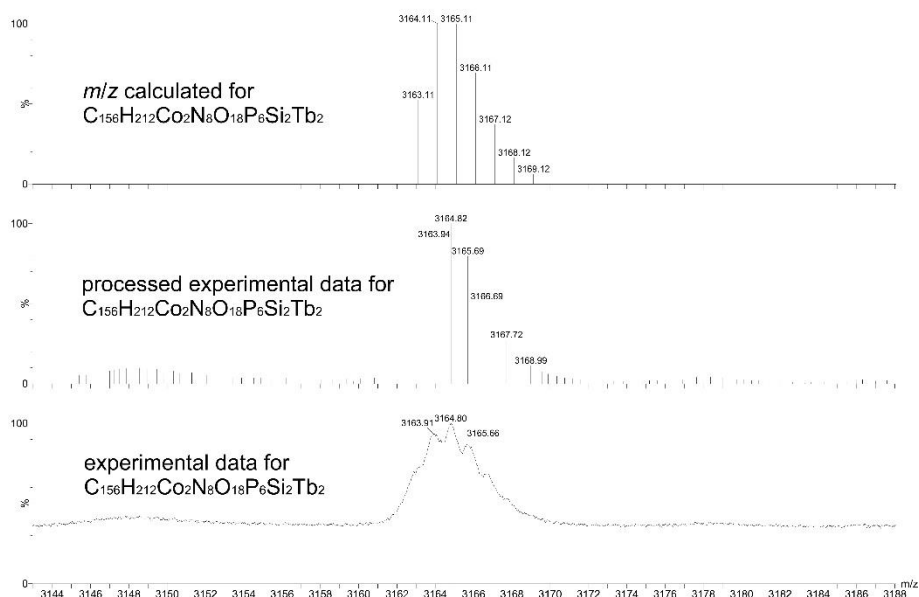


Figure S17. Zoom-in of the MALDI-MS spectrum of P2Tb_2 ($m/z = 3165$ ($\text{C}_{156}\text{H}_{212}\text{Co}_2\text{N}_8\text{O}_{18}\text{P}_6\text{Si}_2\text{Tb}_2$, M^+ requires 3165), matrix: dithranol).

P1Dy

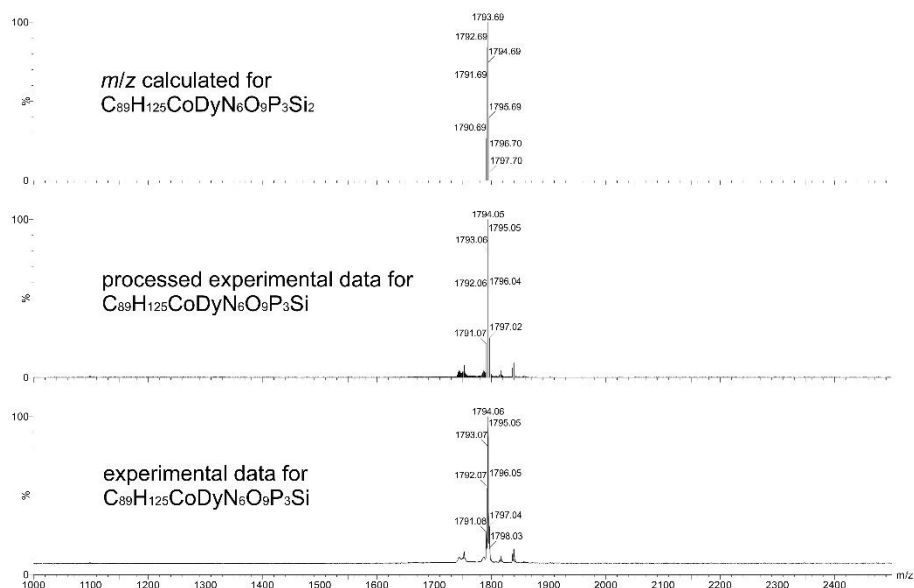


Figure S18. The full MALDI-MS spectrum of P1Dy ($m/z = 1794$ ($\text{C}_{89}\text{H}_{125}\text{CoDyN}_6\text{O}_9\text{P}_3\text{Si}_2$, M^+ requires 1794), matrix: dithranol).

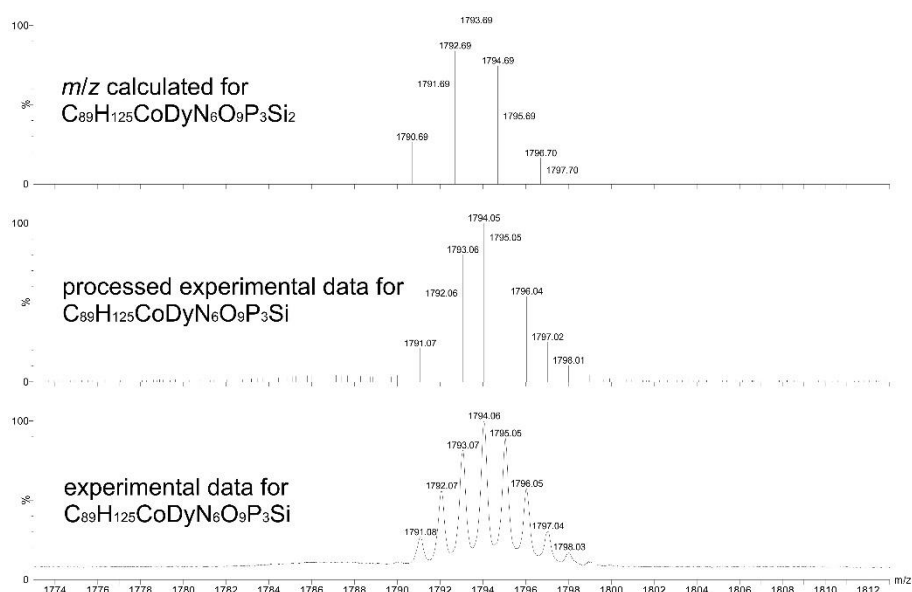


Figure S19. Zoom-in of the MALDI-MS spectrum of **P1_{Dy}** ($m/z = 1794$ ($C_{89}H_{125}CoDyN_6O_9P_3Si_2$, M^+ requires 1794), matrix: dithranol).

P1'_{Dy}

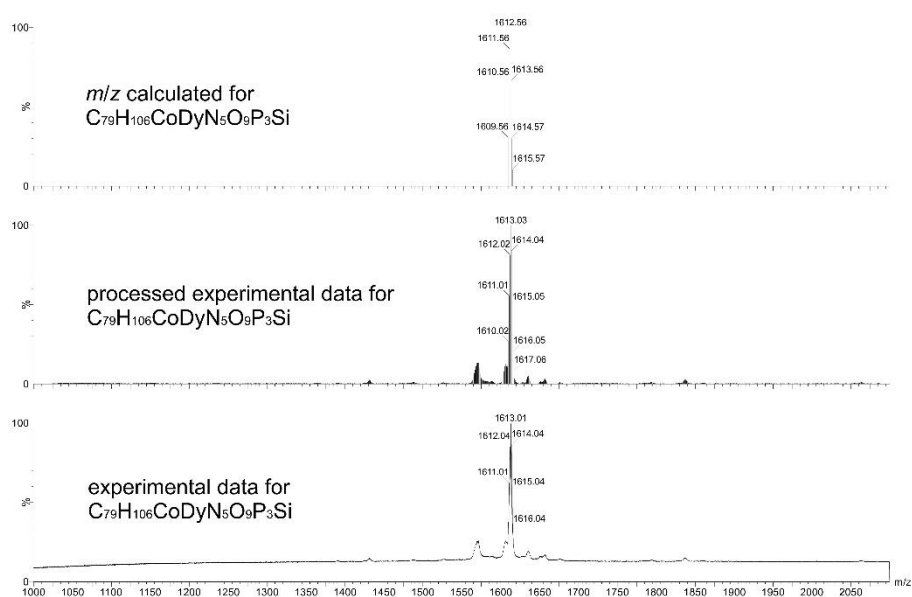


Figure S20. The full MALDI-MS spectrum of **P1'_{Dy}** ($m/z = 1613$ ($C_{79}H_{106}CoDyN_5O_9P_3Si$, M^+ requires 1613), matrix: dithranol).

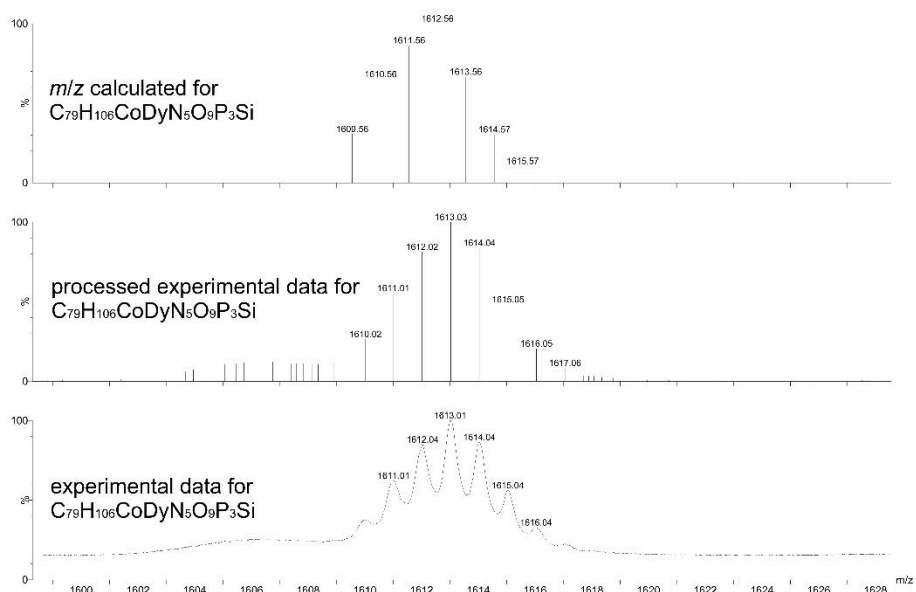


Figure S21. Zoom-in of MALDI-MS spectrum of $P1'Dy$ ($m/z = 1613$ ($C_{79}H_{106}CoDyN_5O_9P_3Si$, M^+ requires 1613), matrix: dithranol).

$P2_{Dy-Tb}$

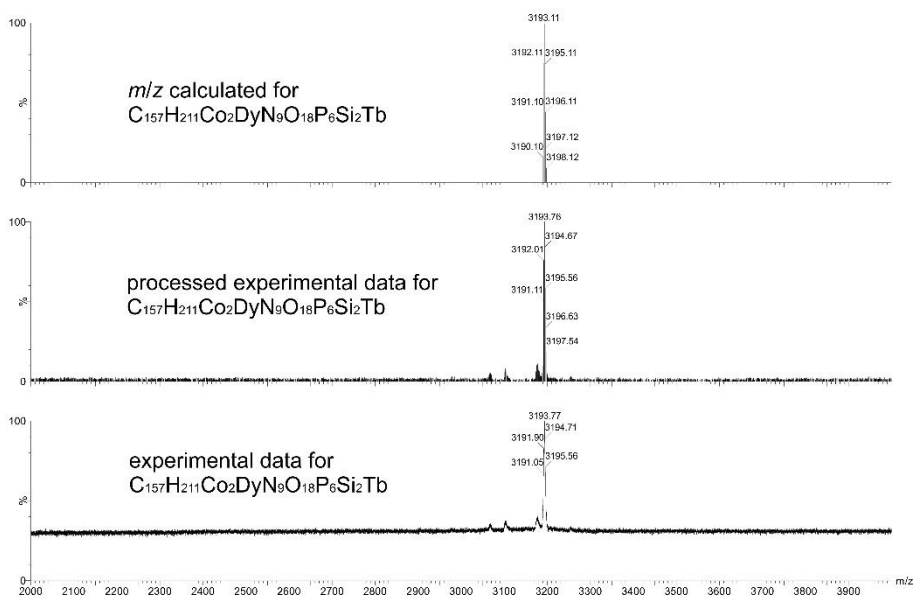


Figure S22. The full MALDI-MS spectrum of $P2_{Dy-Tb}$ ($m/z = 3194$ ($C_{157}H_{211}Co_2DyN_9O_{18}P_6Si_2Tb$, M^+ requires 3193), matrix: dithranol).

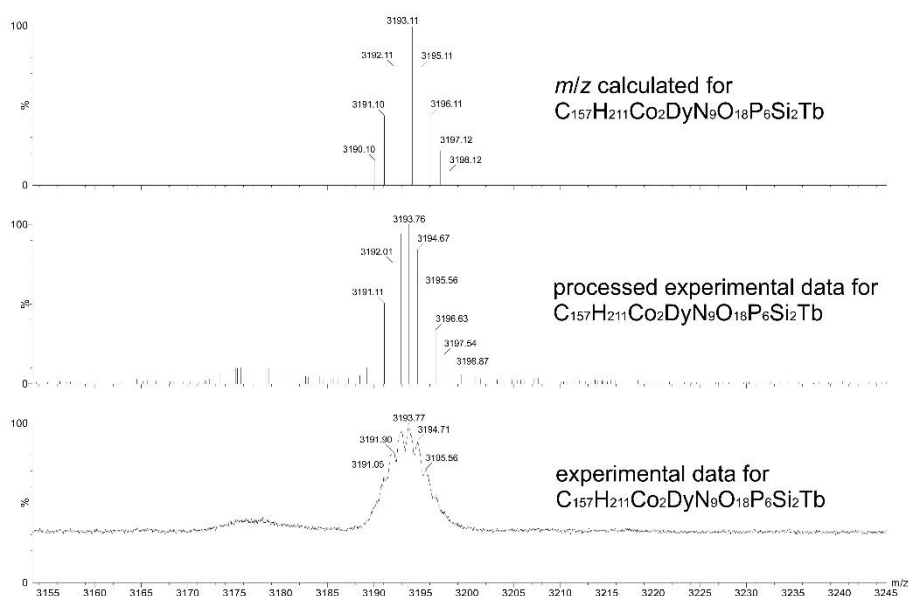


Figure S23. Zoom-in of the MALDI-MS spectrum of **P2_{Dy-Tb}** ($m/z = 3194$ ($C_{157}H_{211}CO_2DyN_9O_{18}P_6Si_2Tb$, M^+ requires 3193), matrix: dithranol).

1.4 UV-vis-NIR Spectroscopy

UV-vis-NIR spectra were recorded of the lanthanide monomers and dimers showing only marginal changes in the absorption spectra across the lanthanide series. The comparability of the spectra indicates the purity of the compounds.

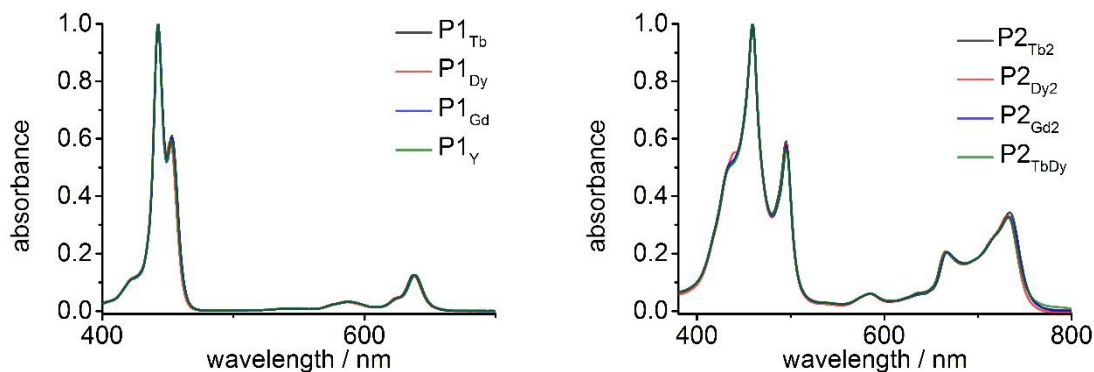


Figure S24. Normalized UV-vis-NIR spectra of **P1_{Ln}** and **P2_{Ln}** ($CHCl_3$, 298K) showing only marginal differences across the lanthanide series.

A slight red-shift in the B-band is observed when comparing a zinc porphyrin monomers and dimers with their terbium analogue.

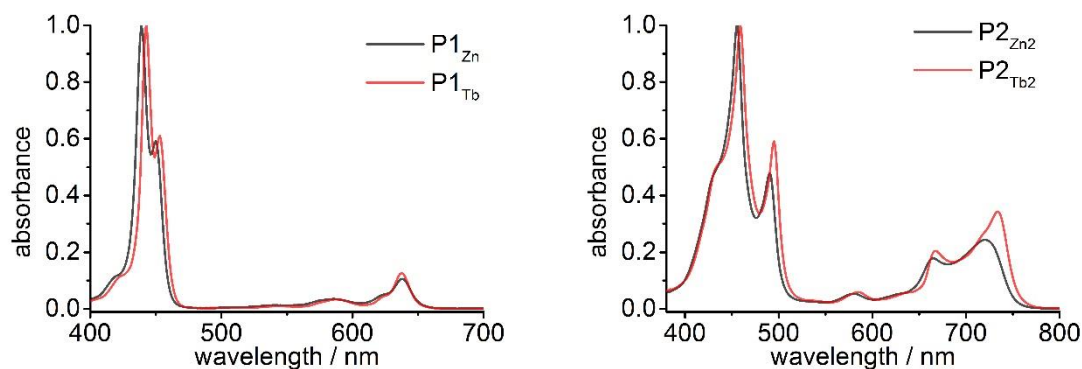


Figure S25. Normalized UV-vis-NIR spectra comparing **P1_{Zn}** with **P1_{Tb}** and **P2_{Zn2}** with **P2_{Tb2}** (CHCl₃, 298K).

2 X-ray Diffraction

2.1 General Experimental Details

A suitable crystal for each sample was selected, mounted on a MITIGEN holder in oil and data collected following a standard method.⁷ Samples **P1'_{Dy}**, **P1_{Dy}**, **P1_{Gd}**, **P1*_{2H}**, **P1*_{Dy}**, **P1_{Zn}**, **P2_{Dy2}** and **P2_{Tb2}** were run on a Rigaku FRE+ diffractometer equipped with HF Varimax confocal mirrors (100µm focus) and an AFC12 goniometer and HG Saturn 724+ detector. Samples **P1*_{Zn}**, **P2_{Gd2}** and **P1_{2H}** were run on a Rigaku FRE+ diffractometer equipped with VHF Varimax confocal mirrors (70µm focus) and an AFC12 goniometer and HG Saturn 724+ detector. Sample **P1_{Tb}** was run on a Rigaku FRE+ diffractometer equipped with VHF Varimax confocal mirrors (70µm focus) and an AFC12 goniometer and HyPix-6000 detector. Sample **P1_Y** was run on a Rigaku 007HF diffractometer equipped with Varimax confocal mirrors and an AFC11 goniometer and HyPix-6000 detector. Cell determination and data collection were carried out using CrystalClear⁸ (**P1'_{Dy}**, **P1*_{Zn}**, **P1_{Zn}**, **P2_{Dy2}**, **P2_{Gd2}** and **P1_{2H}**) or CrysAlisPro⁹ (**P1_{Dy}**, **P1_{Gd}**, **P1*_{2H}**, **P1*_{Dy}**, **P1_{Tb}**, **P1_Y** and **P2_{Tb2}**). With the data reduction, cell refinement and absorption correction using CrysAlisPro⁹. Using Olex2¹⁰, the structures were solved with either *SUPERFLIP*¹¹ (**P1_{2H}**), ShelXD¹² (**P1_{Gd}**) or ShelXT¹³ (the rest) structure solution programs and the models were refined with version 2014/7 of ShelXL¹⁴ using Least Squares minimisation. Hydrogen atom positions were calculated geometrically and refined using the riding model. CDC1565176-1565188 contains supplementary X-ray crystallographic data. This data can be obtained free of charge via <http://www.ccdc.cam.ac.uk/conts/retrieving.html>, or from the Cambridge Crystallographic Data.

2.2 Structures

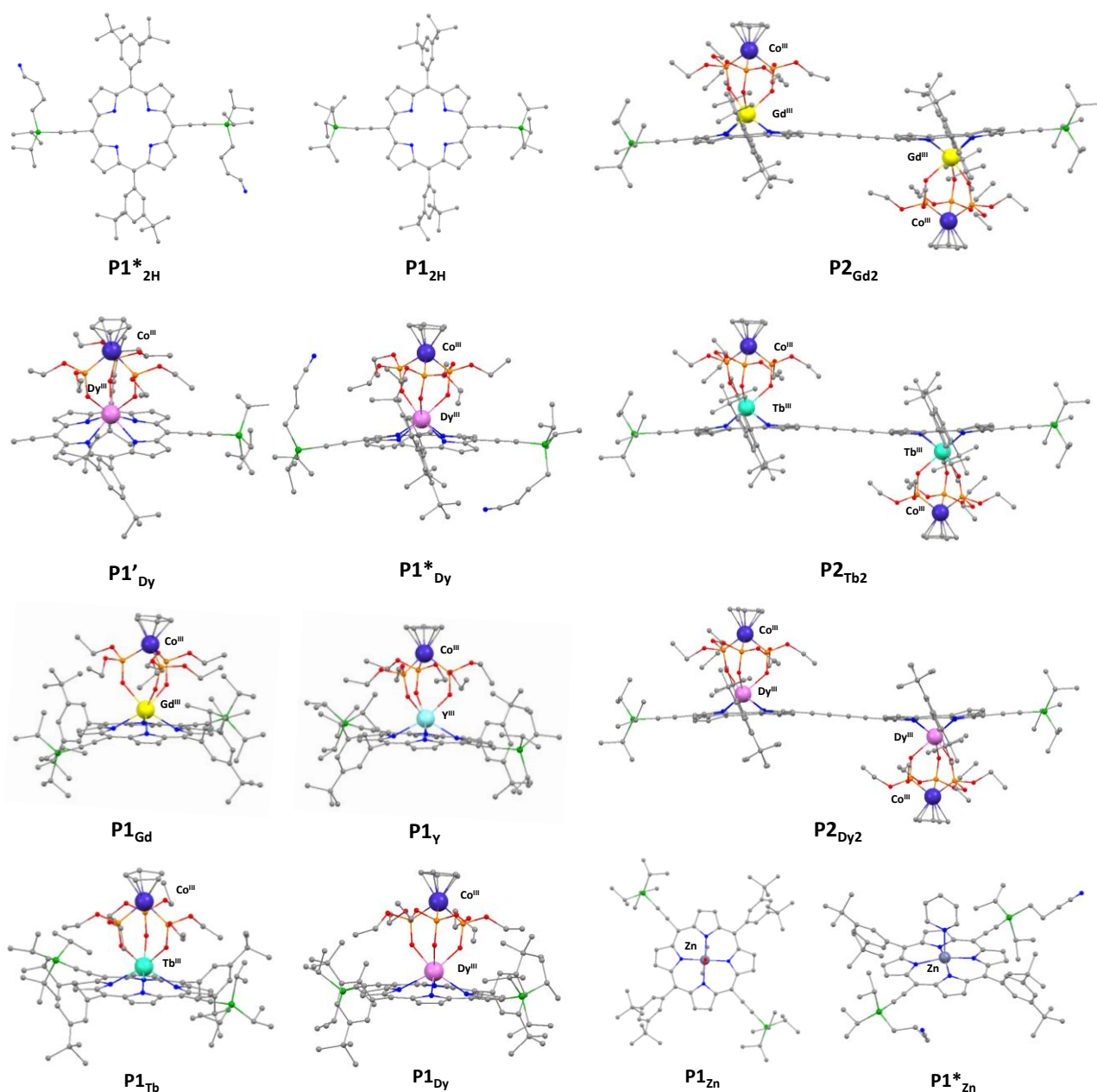


Figure S26. Solid state structures. H atoms and solvent molecules have been removed for clarity. Colour scale: Carbon (grey), oxygen (red), nitrogen (dark blue), phosphorous (orange), cobalt^{III} (purple), dysprosium^{III} (pink), gadolinium^{III} (yellow), terbium^{III} (turquoise), yttrium^{III} (light blue), zink (blue-gray).

2.3 Crystallographic Data

Name	P1 _{2H}	P1* _{2H}	P1' _{Dy}	P1* _{Dy}	P1 _{Dy}
CCDC no.	1565183	1565176	1565185	1565181	1565178
Formula	C ₇₀ H ₉₄ N ₄ Si ₂	C ₇₂ H ₉₂ N ₆ Si ₂	C ₇₈ H ₁₀₇ CoDyN ₄ O ₉ P ₃ Si	C ₈₉ H ₁₂₅ CoDyN ₆ O ₉ P ₃ Si ₂	C ₈₇ H ₁₂₇ CoDyN ₄ O ₉ P ₃ Si ₂
<i>D</i> _{calc.} / g cm ⁻³	1.107	1.145	1.333	1.287	1.257
μ /mm ⁻¹	0.099	0.102	1.279	1.114	1.116
Formula Weight	1047.67	1097.69	1587.10	1793.46	1743.44
Colour	dark blue	Iridescent dark blue	iridescent blue	dark purple	pale dark blueish green
Shape	blade	plate	cut blade	plate	plate
Size/mm ³	0.130×0.050×0.010	0.389×0.209×0.017	0.100×0.050×0.035	0.180×0.100×0.015	0.296×0.142×0.034
<i>T</i> /K	100(2)	100(2)	100(2)	100(2)	100(2)
Crystal System	triclinic	triclinic	monoclinic	triclinic	triclinic
Space Group	P-1	P-1	P2 ₁ /c	P-1	P-1
<i>a</i> /Å	10.7410(11)	10.4966(5)	19.34446(16)	16.1981(3)	16.1487(3)
<i>b</i> /Å	11.0043(11)	12.3975(8)	39.8242(4)	23.3852(4)	19.0993(3)
<i>c</i> /Å	15.1711(14)	13.2265(10)	20.5371(2)	25.4730(5)	30.5159(5)
α /°	69.405(9)	104.289(6)	90	73.821(2)	98.3820(10)
β /°	70.878(9)	99.208(5)	90.4603(9)	89.254(2)	92.0630(10)
γ /°	76.429(9)	101.826(5)	90	86.9650(10)	97.5590(10)
<i>V</i> /Å ³	1571.4(3)	1591.78(18)	15820.8(3)	9253.9(3)	9215.9(3)
<i>Z</i>	1	1	8	4	4
<i>Z'</i>	0.5	0.5	2	2	2
Radiation type	MoK α	MoK α	MoK α	MoK α	MoK α
θ _{min} /°	2.167	2.306	1.468	2.086	2.365
θ _{max} /°	25.027	25.026	27.483	27.486	27.560
Measured Refl.	22040	27097	163836	201316	64909
Independent Refl.	5522	5633	36158	42360	64909
Reflections Used	3733	4022	27568	33616	57464
<i>R</i> _{int}	0.0885	0.0828	0.0618	0.0767	.
Parameters	355	399	2201	2472	2124
Restraints	0	8	2414	5794	5367
Largest Peak	0.931	0.757	2.199	4.089	2.187
Deepest Hole	-0.392	-0.489	-0.956	-1.366	-2.050
Goof	1.034	1.024	1.082	1.117	1.090
<i>wR</i> ₂ (all data)	0.2183	0.2053	0.1387	0.1815	0.1267
<i>wR</i> ₂	0.1940	0.1820	0.1289	0.1694	0.1236
<i>R</i> ₁ (all data)	0.1126	0.1048	0.0830	0.1020	0.0626
<i>R</i> ₁	0.0738	0.0734	0.0588	0.0782	0.0530

Name	P1 _{Gd}	P1 _Y	P1 _{Tb}	P2 _{Gd2}
CCDC no.	1565179	1565184	1565180	1565188
Formula	C ₈₇ H ₁₂₇ CoGdN ₄ O ₉ P ₃ Si ₂	C ₈₇ H ₁₂₇ CoN ₄ O ₉ P ₃ Si ₂ Y	C _{88.5} Cl ₃ CoH ₁₃₀ N ₄ O ₉ P ₃ Si ₂ Tb	C ₁₅₆ H ₂₁₂ Co ₂ Gd ₂ N ₈ O ₁₈ P ₆ Si ₂
<i>D</i> _{calc.} / g cm ⁻³	1.280	1.240	1.314	1.361
<i>μ</i> /mm ⁻¹	1.047	3.517	1.134	1.202
Formula Weight	1738.19	1669.85	1867.25	3161.68
Colour	dark green	dark purple	iridescent purple	green
Shape	plate	opaque prism	plate	plate
Size/mm ³	0.180×0.120×0.035	0.190×0.110×0.060	0.319×0.280×0.041	0.190×0.060×0.005
<i>T</i> /K	100(2)	100(2)	100(2)	100(2)
Crystal System	monoclinic	monoclinic	monoclinic	triclinic
Space Group	Cc	P2 ₁ /c	P2 ₁ /c	P-1
<i>a</i> /Å	16.25392(13)	18.2660(3)	31.5498(4)	10.3106(2)
<i>b</i> /Å	38.80173(18)	14.9061(2)	16.09500(10)	14.6582(3)
<i>c</i> /Å	16.36512(11)	33.9132(5)	19.4714(2)	27.9536(4)
<i>α</i> /°	90	90	90	75.075(2)
<i>β</i> /°	119.1056(10)	104.4550(10)	107.3060(10)	86.248(2)
<i>γ</i> /°	90	90	90	70.983(2)
<i>V</i> /Å ³	9017.84(13)	8941.4(2)	9439.85(17)	3858.65(13)
<i>Z</i>	4	4	4	1
<i>Z'</i>	1	1	1	0.5
Radiation type	MoK _α	CuK _α	MoK _α	MoK _α
<i>θ</i> _{min} /°	2.849	3.183	1.852	2.167
<i>θ</i> _{max} /°	27.482	70.075	27.485	27.484
Measured Refl.	199380	93429	315944	88673
Independent Refl.	20662	16790	21622	17691
Reflections Used	20621	15304	17246	15807
<i>R</i> _{int}	0.0273	0.0361	0.0656	0.0490
Parameters	1266	1275	1228	1015
Restraints	4110	1416	3508	1386
Largest Peak	0.668	1.360	1.928	3.623
Deepest Hole	-0.451	-0.601	-1.148	-1.068
GooF	1.086	1.061	1.048	1.153
<i>wR</i> ₂ (all data)	0.0477	0.1075	0.2681	0.1555
<i>wR</i> ₂	0.0477	0.1050	0.2518	0.1512
<i>R</i> ₁ (all data)	0.0191	0.0438	0.1022	0.0738
<i>R</i> ₁	0.0191	0.0401	0.0872	0.0645
Flack Parameter	0.498(4)			
Hooft Parameter	0.4963(7)			

Name	P2 _{Tb2}	P2 _{Dy2}	P1 _{Zn}	P1* _{Zn}
CCDC no.	1565186	1565182	1565187	1565177
Formula	C ₁₅₆ H ₂₁₂ Co ₂ N ₈ O ₁₈ P ₆ Si ₂ Tb ₂	C ₁₅₆ H ₂₁₂ Co ₂ Dy ₂ N ₈ O ₁₈ P ₆ Si ₂	C ₇₄ H ₁₀₈ N ₄ O ₄ Si ₂ Zn	C _{77.5} H ₉₆ ClN ₇ Si ₂ Zn
<i>D</i> _{calc.} / g cm ⁻³	1.360	1.380	1.148	1.193
μ /mm ⁻¹	1.257	1.325	0.424	0.462
Formula Weight	3165.02	3172.18	1239.19	1282.61
Colour	green	green	iridescent purple	iridescent blue-green
Shape	plate	plate	block	plate
Size/mm ³	0.210×0.080×0.010	0.170×0.110×0.005	0.130×0.110×0.070	0.250×0.065×0.015
<i>T</i> /K	100(2)	100(2)	100(2)	100(2)
Crystal System	triclinic	triclinic	monoclinic	triclinic
Space Group	P-1	<i>P</i> -1	P2 ₁ /c	P-1
<i>a</i> /Å	10.30820(10)	10.25340(18)	8.05199(12)	13.1710(4)
<i>b</i> /Å	14.6723(2)	14.6267(3)	13.9466(2)	14.3764(4)
<i>c</i> /Å	27.9524(5)	27.8407(5)	31.9300(5)	19.9456(6)
α /°	75.0610(10)	75.0624(16)	90	90.736(2)
β /°	86.2080(10)	86.2571(15)	90.6300(13)	91.970(2)
γ /°	71.1390(10)	71.1737(16)	90	108.933(3)
<i>V</i> /Å ³	3864.76(10)	3817.71(13)	3585.47(9)	3569.14(19)
<i>Z</i>	1	1	2	2
<i>Z</i> '	0.5	0.5	0.5	1
Radiation type	MoK α	MoK α	MoK α	MoK α
θ _{min} /°	2.207	2.166	2.846	2.504
θ _{max} /°	27.486	27.484	27.485	27.485
Measured Refl.	85977	80838	48760	57370
Independent Refl.	17755	17496	8193	16242
Reflections Used	16997	15823	7373	11197
<i>R</i> _{int}	0.0515	0.0415	0.0296	0.0631
Parameters	1197	1052	403	897
Restraints	2917	1033	3	986
Largest Peak	2.043	1.818	1.338	1.161
Deepest Hole	-2.319	-1.070	-0.408	-0.904
GooF	1.278	1.102	1.092	1.035
<i>wR</i> ₂ (all data)	0.1316	0.1126	0.1710	0.2218
<i>wR</i> ₂	0.1302	0.1096	0.1669	0.1989
<i>R</i> ₁ (all data)	0.0659	0.0575	0.0629	0.1224
<i>R</i> ₁	0.0625	0.0499	0.0575	0.814

2.4 Continuous Shape Measure

The Continuous Shape Measures (CShM) software¹⁵ was used to evaluate how close the polyhedral surrounding each lanthanide deviates from the ideal shape. The coordination polyhedron with the lowest CShM value defines the best polyhedron. Values larger than 0.1 are considered chemically significant distortions while values larger than about 3 indicate important distortions.

Below is the CShM for the coordination polyhedra of each lanthanide in the structure of complex **P1_{Dy}**, **P2_{Dy2}**, **P1_{Tb}**, **P2_{Tb2}**, **P1_{Gd}**, **P2_{Gd2}** compared to known 7-vertex polyhedral.

	Heptagon (D7h)	Hexagonal pyramid (C6v)	Pentagonal bipyramid (D5h)	Capped octahedron (C3v)	Capped trigonal prism (C2v)	Johnson pentagonal bipyramid J13 (D5h)	Johnson elongated triangular pyramid J7 (C3v)
P1_{Dy(a)_1}	35.378	19.198	6.035	0.814	0.82	9.728	20.895
P1_{Dy(a)_2}	36.331	18.432	7.138	1.634	0.956	10.975	20.998
P1_{Dy(b)}	35.853	19.252	6.38	0.281	1.717	10.009	20.636
P2_{Dy2_1}	35.915	19.275	5.861	0.524	1.635	9.706	20.612
P2_{Dy2_2}	34.903	19.598	6.208	0.766	1.076	9.712	19.46
P1_{Tb_1}	36.323	18.778	5.842	0.681	1.611	9.838	20.555
P1_{Tb_2}	36.368	18.741	6.489	1.278	1.126	10.276	21.01
P2_{Tb2_1}	35.824	19.128	5.916	0.554	1.696	9.777	20.727
P2_{Tb2_2}	34.871	19.453	6.217	0.73	1.235	9.744	19.547
P1_{Gd_1}	34.669	19.377	6.97	1.262	0.637	10.675	20.939
P1_{Gd_2}	35.068	19.305	6.676	1.8	0.895	10.681	20.251
P1_{Gd_3}	35.418	18.713	6.241	1.117	0.95	10.368	20.749
P2_{Gd2_1}	35.664	19.153	5.919	0.563	1.736	9.743	20.628
P2_{Gd2_2}	34.764	19.357	6.257	0.743	1.268	9.823	19.64

* **P1_{Dy(a)}**/**P1_{Dy(b)}** represent the two different molecules present in the asymmetric unit for **P1_{Dy}**. The **_1**, **_2** and **_3** represent the different parts of disorder of the phosphine ligands in the molecules.

3 Squid Measurements

3.1 Experimental Details

For all samples, SQUID analyses were performed on crushed polycrystalline samples wrapped in a polyethylene membrane. The direct current (dc) magnetic susceptibility measurements were obtained using a Quantum Design SQUID magnetometer MPMS-XL7. Dc measurements were taken in the temperature range of 1.8 and 300 K for fields ranging from -7 to 7 T. For the Dy and Tb-containing samples alternating current (ac) magnetic susceptibility measurements were carried out under an oscillating ac field of 4 Oe and ac frequencies ranging from 1 to 1500 Hz. Diamagnetic corrections were applied for the sample holder and for the core diamagnetism from the sample, calculated from Pascal constants.

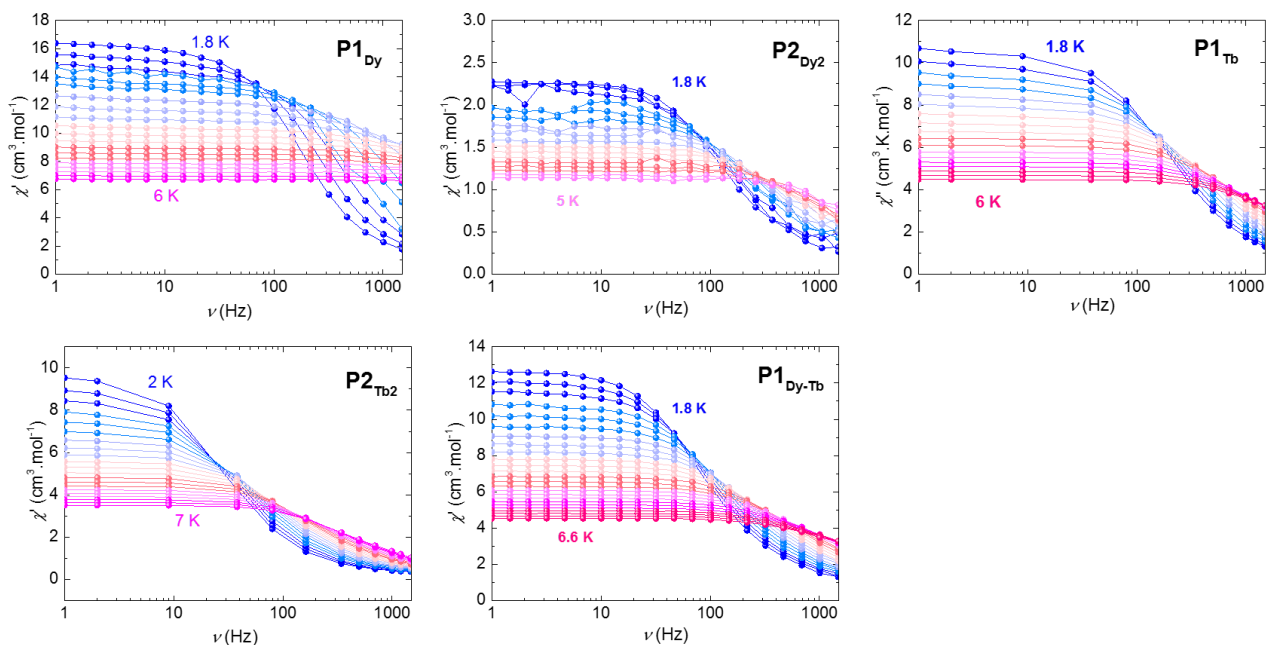


Figure S27. In-phase (χ') magnetic susceptibility of **P1_{Dy}**, **P2_{Dy2}**, **P1_{Tb}**, **P2_{Tb2}**, and **P1_{Dy-Tb}**. All measurements were taken crushed polycrystalline samples under an applied dc field of 2000 Oe and an ac field of 4 Oe.

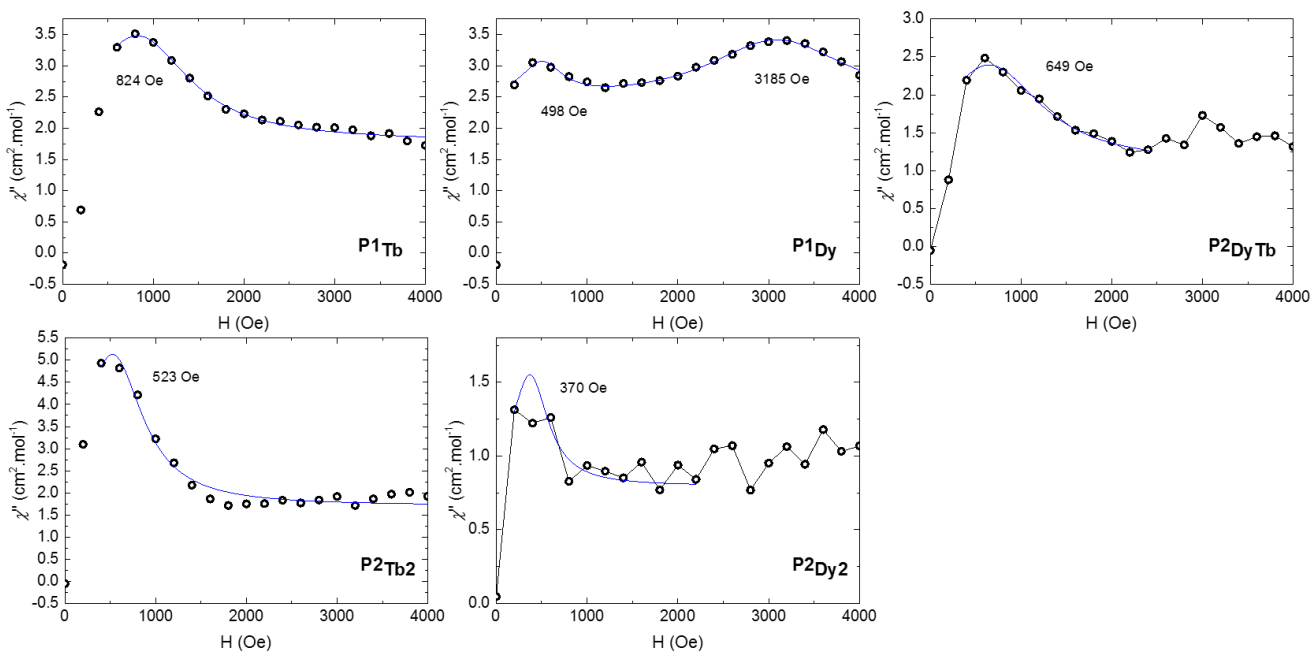


Figure S28. Variable field χ'' magnetic susceptibility of **P1_{Tb}**, **P2_{Tb2}**, **P1_{Dy}**, **P2_{Dy2}** and **P2_{Dy-Tb}** at 2 K and 1500 Hz. The blue line is a Lorenz Fit to the data. As expected we see 2 peaks in the field dependence of **P1_{Dy}**, one for each of the two molecules in the asymmetric.

4 Electron Paramagnetic Resonance Spectroscopy

4.1 Methods

EPR data were collected in the Centre for Advanced ESR (CAESR) in the Department of Chemistry, University of Oxford. All X-band data were obtained on a Bruker EleXsys E680. Q-band data was acquired using a Bruker EleXsys E580. An Oxford Instruments CF9350 cryostat was used to maintain the sample temperature and an Oxford Instruments ITC503 to control it. As microwave resonators, we used a Bruker ER4118X-MS3-W1 on the EleXsys E680 and Bruker EN510702 on the EleXsys E580. Magnetic fields were generated with an electromagnet. For measurements at X-band frequency, the sample was dissolved with a concentration of 1 mmol/l in Toluene/Dichloromethane (1:1). For Q-band frequency, we prepared a 1 mmol/l solution in Acetonitrile/2-Methyltetrahydrofuran.

FID-detected absorption spectra

Free induction decay (FID)-detected absorption spectra were obtained by excitation of the system with a long π -pulse (800 ns). Therefore, a FID signal can be recorded after the receiver protection switch. Measurements were performed at cryogenic temperatures which enables a strong signal.

Phase-memory and quantum coherence times

The phase-memory time was obtained using a Hahn-echo sequence, $\pi/2 - \tau - \pi - \tau - \text{echo}$. A $\pi/2$ -pulse turns the spin orientation into the xy-plane, where they start to interact freely. During this evolution period, the spins interact with their environment (such as nuclear spin bath or spin-spin interactions) and begin to dephase. After a time-delay τ , we apply a π -pulse and thus after another time τ , spins recombine and yield a signal intensity (echo). Since decoherence occurs over both periods of τ , the data is fit with a dependence of the signal intensity versus time 2τ using

$$Y(\tau) = Y_0 e^{-\left(\frac{2\tau}{T_m}\right)^x},$$

where Y corresponds to the signal intensity, T_m to the phase-memory time and x is a stretching factor to account for the composition of the factors that influence dephasing. At Q-band frequency, we used pulse durations of 16 ns and 32 ns for the $\pi/2$ and π pulses, respectively. The magnetic field at Q-band frequency was set to 1281.3 mT. At X-band frequency, we used longer pulse durations of 500 ns and 1000 ns for the $\pi/2$ and π pulses, respectively, to remove modulation effects in the spectrum.

Spin-lattice relaxation times

The spin-lattice relaxation time T_1 was obtained using the inversion recovery technique, $\pi - t - \pi/2 - \tau - \pi - \tau - \text{echo}$. A π -pulse flips the orientation of the spins, and after a time t the recovered spin intensity is measured with a Hahn-echo sequence as shown above. Data was fitted using a sum of two exponential functions to account for spectral diffusion. The part with the larger value of T_1 was identified to be related with spin-lattice relaxation. We used pulse durations of 16 ns and 32

ns for the $\pi/2$ and π pulses, respectively, and a fixed dephasing time of $\tau = 300$ ns. Magnetic field at Q-band frequency was set to 1281.3 mT.

4.2 Q-band spectrum

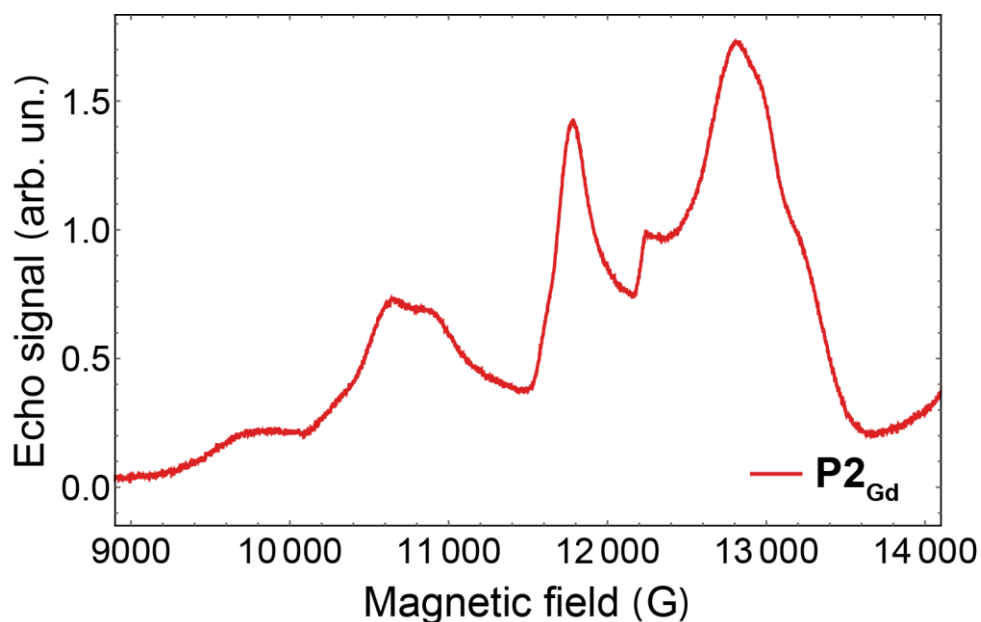


Figure S29. Central EPR transitions within the FID-detected absorption spectrum of $P2Gd_2$ at Q-band frequency (33.9926 GHz) and 10 K, from integrating the FID of a 800 ns pulse.

4.3 Spin-lattice relaxation at Q-band frequency

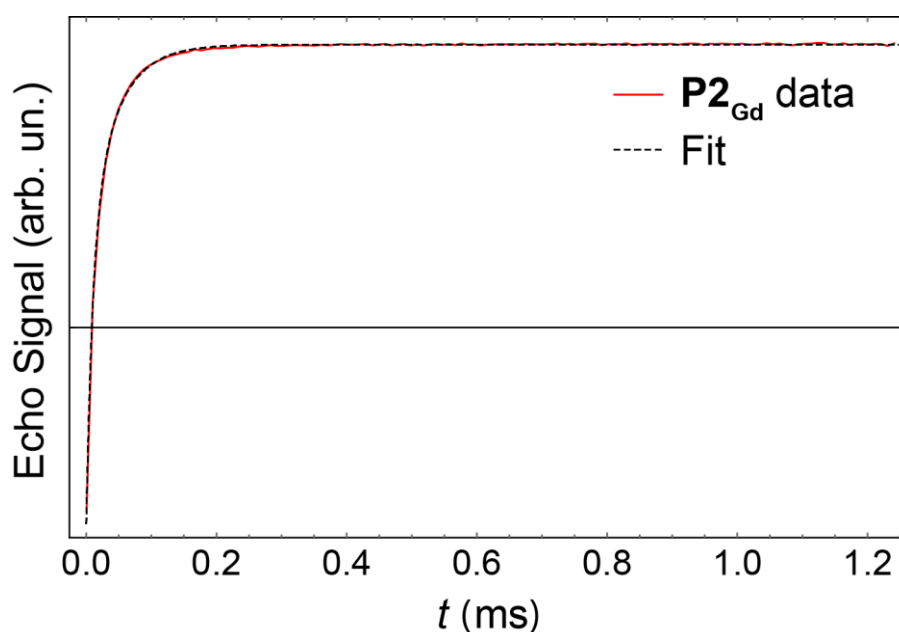


Figure S30. Inversion recovery behavior of $P2Gd_2$ at Q-band frequency (≈ 34 GHz), 10 K and 1281.3 mT. The fitted relaxation times are 10.0 μ s and 43.4 μ s, accounted for spectral diffusion and spin-lattice relaxation time T_1 , respectively.

4.4 Phase-Memory Time T_m at Q-band frequency

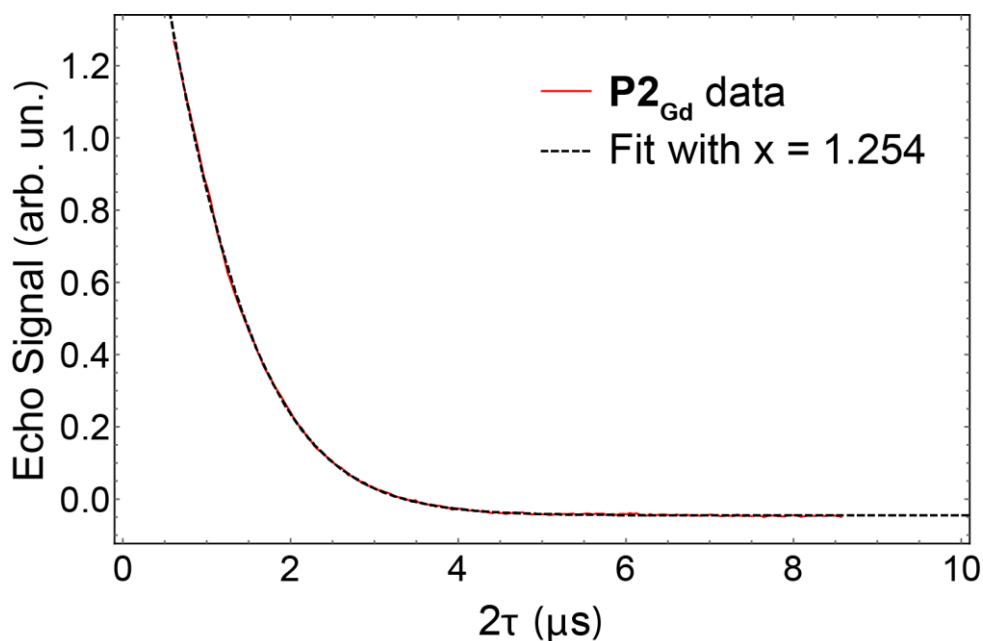


Figure S31. Echo signal after the Hahn-echo sequence of $\mathbf{P2}_{\text{Gd}2}$ at Q-band frequency (≈ 34 GHz), 10 K and 1281.3 mT. We found $x = 1.254$ and $T_m = 2297$ ns. A slightly worse, but better comparable fit is obtained when the stretch factor is fixed to 1, giving $T_m = 1786$ ns.

4.5 Quantum coherence times versus field at X-band frequency

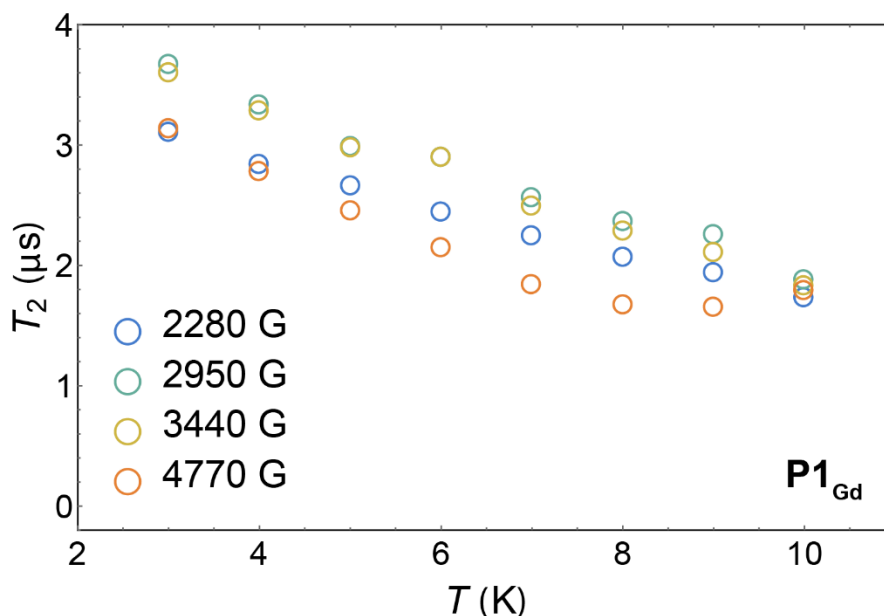


Figure S32. Obtained quantum coherence times T_2 for $\mathbf{P1}_{\text{Gd}}$ at different magnetic fields and different temperatures at X-band frequency (≈ 9.5 GHz).

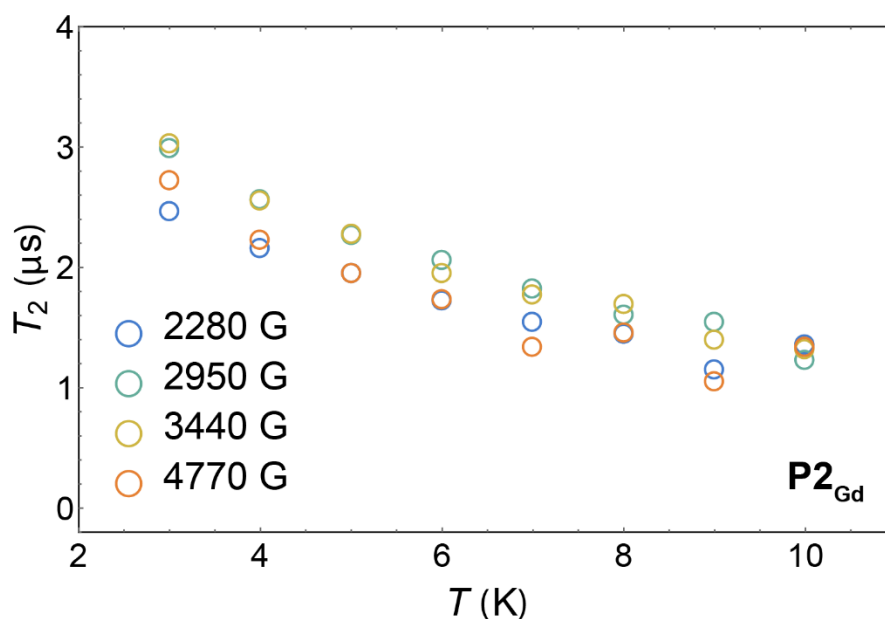


Figure S33. Obtained quantum coherence times T_2 for P2Gd_2 at different magnetic fields and different temperatures at X-band frequency (≈ 9.5 GHz).

5 References

- (1) M. J. Plater, S. Aiken and G. Bourhill, *G. Tetrahedron*, 2002, **58**, 2405.
- (2) M. J. Plater, S. Aiken and G. Bourhill, *Tetrahedron*, 2002, **58**, 2415.
- (3) V. Harder, E. Dubler and H. Werner, *J. Organomet. Chem.*, 1974, **71**, 427.
- (4) F. Gao, M.-X. Yao, Y.-Y. Li, Y.-Z. Li, Y. Song and J.-L. Zuo, *Inorg. Chem.*, 2013, **52**, 6407.
- (5) W. Kläui, H. Neukomm, H. Werner, G. Huttner, *Chem. Ber.*, 1977, **110**, 2283.
- (6) W. Kläui, *Angew. Chem. Int. Ed.*, 1990, **29**, 627.
- (7) S. J. Coles and P. A. Gale, *Chem. Sci.*, 2012, **3**, 683.
- (8) Rigaku, *CrystalClear- SM Expert 3.1 b27*, **2013**.
- (9) CrysAlisPro Software System, Rigaku Oxford Diffraction, Yarnton, Oxford, UK, **2015**.
- (10) O. V. Dolomanov, L. J. Bourhis, R. J. Gildea, J. A. K. Howard, H. Puschmann, *J. Appl. Cryst.*, 2009, **42**, 339.
- (11) L. Palatinus and G. Chapuis, *J. Appl. Cryst.*, 2007, **40**, 786.
- (12) G. M. Sheldrick, *Acta. Cryst.*, 2008, **A64**, 339.
- (13) G. M. Sheldrick, *Acta. Cryst.*, 2015, **A71**, 3.
- (14) G. M. Sheldrick, *Acta. Cryst.*, 2015, **C27**, 3.
- (15) M. Llunell, D. Casanova, J. Girera, P. Alemany, S. Alvarez, SHAPE, Continuous Shape Measures Calculation, version 2.0; Universitat de Barcelona: Barcelona, Spain, 2010.